

**Imperial College
London**

IMPERIAL COLLEGE LONDON
DEPARTMENT OF MATHEMATICS

**Deep Hedging under Reweighted
Asset Measure**

Author: Winter Shi (CID: 01256799)

A thesis submitted for the degree of
MSc in Mathematics and Finance, 2020-2021

Declaration

The work contained in this thesis is my own work unless otherwise stated.

Date: September 7, 2021

Acknowledgements

I would like to thank my supervisor Dr Mikko Pakkanen for his selfless support in taking this research topic and for providing guidance as the research progressed, especially in the difficult situation this year. His feedback was invaluable in determining further results to be pursued and improvements on research structure, particularly when the new results have emerged and the research goals have evolved.

I would also like to express my deepest appreciation to all of the lecturers in the MSc Mathematics and Finance course at Imperial College London, for providing great supports and making the course content relevant.

Finally, my special gratitude goes to my family who always stands by my side and my friends, the old ones and the new ones, for making this year one to remember.

Abstract

The adoption of artificial intelligence methods in the financial industry widens the door to data-driven decision-making, algorithmic trading, etc. In this paper, a method called deep hedging with reweighted measure is introduced. The normal deep hedging represents hedging price data with a single feedforward neural network. It helps to reduce parameters of deep learning comparing with a strategy using multiple networks for different time steps. The deep hedging with reweighted measure improves the deep hedging from replacing the traditional loss function by an exponential utility function and reweighting the probability measure for each asset path for making the underlying asset price free of arbitrage. This method improves the resulted hedging strategy, especially for markets with large monotonic price increments, and have multiple financial applications.

Contents

1	Introduction	9
2	Pricing models	11
2.1	Black-Scholes Model	11
2.1.1	Black-Scholes European Option Pricing	12
2.1.2	Girsanov's Theorem	12
2.1.3	Delta Hedging	14
2.2	Heston Model	16
2.2.1	Characteristic Function	17
2.2.2	Unreliable Delta Hedging	18
3	Feedforward Neural Network (FNN)	19
3.1	General Construction	19
3.2	Activation Functions	20
3.3	Loss Functions	21
4	Pricing and Hedging by Unsupervised Deep Learning	22
4.1	Setting: Discrete Time-market Simulation	22
4.2	Deep Hedging	23
4.3	Exponential Utility Indifference Pricing	26
4.4	Probability Measure Reweighting	27
5	Numerical Results	29
5.1	Deep Hedging and Measure Reweighting in Black-Scholes Model	29
5.2	Deep Hedging and Measure Reweighting in Heston Model	39
5.3	Black-Scholes Model with Realized Volatility	49
5.4	Pairs Trading on Real Funds	51
6	Conclusion	54
A	Additional Figures	56
A.1	Figures for Black-Scholes model	56
A.1.1	Figures with $\lambda = 1$	56
A.1.2	Figures with $\lambda = 5$	62
A.2	Figures for Heston model	67
A.2.1	Figures with $\lambda = 1$	67
A.2.2	Figures with $\lambda = 5$	76

List of Figures

4.1	The single feedforward neural network (FNN) illustrated by Horvath et al. [2]. Input #1 is the series of time steps t . Input #2, #3, ..., are the sets containing price paths for one asset. FNN here hedges among these assets and results the corresponding hedging strategies. .	25
5.1	Black-Scholes model - Comparison of hedge ratio between deep hedging strategy with reweighted, Radon-Nikodym and unweighted measure and the delta hedging strategy with drift term $\mu = 0$ at time $t/T = 0.9$	30
5.2	Black-Scholes model - The profit and loss histogram for European call option and hedge ratio for a hedge path among deep hedging strategy with reweighted, Radon-Nikodym and unweighted measure and the delta hedging strategy with drift term $\mu = 0$ and risk aversion $\lambda = 15$	31
5.3	Black-Scholes model - Hedge European call option with $\lambda = 7$ for different positive drift term μ . The graphs are shown with respect to changes in time.	32
5.4	Black-Scholes model - Comparison of the hedge ratio between deep hedging strategy with reweighted, Radon-Nikodym and unweighted measure and the delta hedging strategy with $\lambda = 7$ and $\mu = 0.1$	33
5.5	Black-Scholes model - Comparison of the hedge ratio between deep hedging strategy with reweighted, Radon-Nikodym and unweighted measure and the delta hedging strategy with $\lambda = 7$ and $\mu = 0.3$	33
5.6	Black-Scholes model - Comparison of the hedge ratio between deep hedging strategy with reweighted, Radon-Nikodym and unweighted measure and the delta hedging strategy with $\lambda = 7$ and $\mu = 0.6$	34
5.7	Black-Scholes model - Comparison of the hedge ratio between deep hedging strategy with reweighted, Radon-Nikodym and unweighted measure and the delta hedging strategy with $\lambda = 7$ and $\mu = 1.0$	34
5.8	Black-Scholes model - The underlying asset price histogram simulated by computer with drift term $\mu = 0.1$	35
5.9	Black-Scholes model - The underlying asset price histogram simulated by computer with drift term $\mu = 1$	35
5.10	Black-Scholes model - Hedge European call option with $\lambda = 7$ for different negative drift term μ . The graphs are shown with respect to changes in time.	36
5.11	Black-Scholes model - Comparison of the hedge ratio between deep hedging strategy with reweighted, Radon-Nikodym and unweighted measure and the delta hedging strategy with $\lambda = 7$ and $\mu = -0.1$	37

5.12	Black-Scholes model - Comparison of the hedge ratio between deep hedging strategy with reweighted, Radon-Nikodym and unweighted measure and the delta hedging strategy with $\lambda = 7$ and $\mu = -0.3$. . .	37
5.13	Black-Scholes model - Comparison of the hedge ratio between deep hedging strategy with reweighted, Radon-Nikodym and unweighted measure and the delta hedging strategy with $\lambda = 7$ and $\mu = -0.6$. . .	38
5.14	Black-Scholes model - Comparison of the hedge ratio between deep hedging strategy with reweighted, Radon-Nikodym and unweighted measure and the delta hedging strategy with $\lambda = 7$ and $\mu = -1.0$. . .	38
5.15	Heston model - Hedge European call option with $\mu = 0.1$ and $\lambda = 10$ for different volatility of instantaneous volatility ξ . The graphs are shown with respect to changes in time.	40
5.16	Heston model - Hedge European call option with $\mu = 0.3$ and $\lambda = 10$ for different volatility of instantaneous volatility ξ . The graphs are shown with respect to changes in time.	41
5.17	Heston model - Hedge European call option with $\mu = 0.6$ and $\lambda = 10$ for different volatility of instantaneous volatility ξ . The graphs are shown with respect to changes in time.	42
5.18	Heston model - Hedge European call option with $\mu = 0.1$, $\lambda = 10$ and different positive volatility of instantaneous volatility ξ	43
5.19	Heston model - Hedge European call option with $\mu = 0.1$, $\lambda = 10$ and different negative volatility of instantaneous volatility ξ	44
5.20	Heston model - Hedge European call option with $\mu = 0.3$, $\lambda = 10$ and different positive volatility of instantaneous volatility ξ	45
5.21	Heston model - Hedge European call option with $\mu = 0.3$, $\lambda = 10$ and different negative volatility of instantaneous volatility ξ	46
5.22	Heston model - Hedge European call option with $\mu = 0.6$, $\lambda = 10$ and different positive volatility of instantaneous volatility ξ	47
5.23	Heston model - Hedge European call option with $\mu = 0.6$, $\lambda = 10$ and different negative volatility of instantaneous volatility ξ	48
5.24	Black-Scholes model - Scatter Plot of the standard derivation for underlying asset price (i.e., the realized volatility $\sigma^{realized}$) and the trained reweighted measure	50
5.25	The histogram of profit and loss with reweighted measure and the scatter plot of two funds correlation and their reweighted measure. . .	51
5.26	The scatter plots of two funds correlation (p-value based on MacKinnon [17]) and their different-scaled reweighted measure.	52
5.27	Related price paths of fund VOO and IVV with maturity $T = 2$ min. Data was collected seconds-by-seconds in year 2020	53
5.28	Price path differences between fund VOO and IVV with maturity $T = 2$ min by investing same number of shares. Data was collected seconds-by-seconds in year 2020	53
A.1	Black-Scholes model - Hedge European call option with $\lambda = 1$ for different positive μ . The graphs are shown with respect to changes in time.	56

A.2	Black-Scholes model - Hedge European call option with $\lambda = 1$ for different negative μ . The graphs are shown with respect to changes in time.	57
A.3	Black-Scholes model - Comparison of the hedge ratio between deep hedging strategy with reweighted, Radon-Nikodym and unweighted measure and the delta hedging strategy with $\lambda = 1$ and $\mu = 0.1$. . .	58
A.4	Black-Scholes model - Comparison of the hedge ratio between deep hedging strategy with reweighted, Radon-Nikodym and unweighted measure and the delta hedging strategy with $\lambda = 1$ and $\mu = 0.3$. . .	58
A.5	Black-Scholes model - Comparison of the hedge ratio between deep hedging strategy with reweighted, Radon-Nikodym and unweighted measure and the delta hedging strategy with $\lambda = 1$ and $\mu = 0.6$. . .	59
A.6	Black-Scholes model - Comparison of the hedge ratio between deep hedging strategy with reweighted, Radon-Nikodym and unweighted measure and the delta hedging strategy with $\lambda = 1$ and $\mu = 1.0$. . .	59
A.7	Black-Scholes model - Comparison of the hedge ratio between deep hedging strategy with reweighted, Radon-Nikodym and unweighted measure and the delta hedging strategy with $\lambda = 1$ and $\mu = -0.1$. .	60
A.8	Black-Scholes model - Comparison of the hedge ratio between deep hedging strategy with reweighted, Radon-Nikodym and unweighted measure and the delta hedging strategy with $\lambda = 1$ and $\mu = -0.3$. .	60
A.9	Black-Scholes model - Comparison of the hedge ratio between deep hedging strategy with reweighted, Radon-Nikodym and unweighted measure and the delta hedging strategy with $\lambda = 1$ and $\mu = -0.6$. .	61
A.10	Black-Scholes model - Comparison of the hedge ratio between deep hedging strategy with reweighted, Radon-Nikodym and unweighted measure and the delta hedging strategy with $\lambda = 1$ and $\mu = -1.0$. .	61
A.11	Black-Scholes model - Hedge European call option with $\lambda = 5$ for different positive μ . The graphs are shown with respect to changes in time.	62
A.12	Black-Scholes model - Hedge European call option with $\lambda = 5$ for different negative μ . The graphs are shown with respect to changes in time.	62
A.13	Black-Scholes model - Comparison of the hedge ratio between deep hedging strategy with reweighted, Radon-Nikodym and unweighted measure and the delta hedging strategy with $\lambda = 5$ and $\mu = 0.1$. . .	63
A.14	Black-Scholes model - Comparison of the hedge ratio between deep hedging strategy with reweighted, Radon-Nikodym and unweighted measure and the delta hedging strategy with $\lambda = 5$ and $\mu = 0.3$. . .	63
A.15	Black-Scholes model - Comparison of the hedge ratio between deep hedging strategy with reweighted, Radon-Nikodym and unweighted measure and the delta hedging strategy with $\lambda = 5$ and $\mu = 0.6$. . .	64
A.16	Black-Scholes model - Comparison of the hedge ratio between deep hedging strategy with reweighted, Radon-Nikodym and unweighted measure and the delta hedging strategy with $\lambda = 5$ and $\mu = 1.0$. . .	64
A.17	Black-Scholes model - Comparison of the hedge ratio between deep hedging strategy with reweighted, Radon-Nikodym and unweighted measure and the delta hedging strategy with $\lambda = 5$ and $\mu = -0.1$. .	65

A.18 Black-Scholes model - Comparison of the hedge ratio between deep hedging strategy with reweighted, Radon-Nikodym and unweighted measure and the delta hedging strategy with $\lambda = 5$ and $\mu = -0.3$. . .	65
A.19 Black-Scholes model - Comparison of the hedge ratio between deep hedging strategy with reweighted, Radon-Nikodym and unweighted measure and the delta hedging strategy with $\lambda = 5$ and $\mu = -0.6$. . .	66
A.20 Black-Scholes model - Comparison of the hedge ratio between deep hedging strategy with reweighted, Radon-Nikodym and unweighted measure and the delta hedging strategy with $\lambda = 5$ and $\mu = -1.0$. . .	66
A.21 Heston model - Hedge European call option with $\mu = 0.1$, $\lambda = 1$ and different volatility of instantaneous volatility ξ . The graphs are shown with respect to changes in time.	67
A.22 Heston model - Hedge European call option with $\mu = 0.3$, $\lambda = 1$ and different volatility of instantaneous volatility ξ . The graphs are shown with respect to changes in time.	68
A.23 Heston model - Hedge European call option with $\mu = 0.6$, $\lambda = 1$ and different volatility of instantaneous volatility ξ . The graphs are shown with respect to changes in time.	69
A.24 Heston model - Hedge European call option with $\mu = 0.1$, $\lambda = 1$ and different positive volatility of instantaneous volatility ξ	70
A.25 Heston model - Hedge European call option with $\mu = 0.1$, $\lambda = 1$ and different negative volatility of instantaneous volatility ξ	71
A.26 Heston model - Hedge European call option with $\mu = 0.3$, $\lambda = 1$ and different positive volatility of instantaneous volatility ξ	72
A.27 Heston model - Hedge European call option with $\mu = 0.3$, $\lambda = 1$ and different negative volatility of instantaneous volatility ξ	73
A.28 Heston model - Hedge European call option with $\mu = 0.6$, $\lambda = 1$ and different positive volatility of instantaneous volatility ξ	74
A.29 Heston model - Hedge European call option with $\mu = 0.6$, $\lambda = 1$ and different negative volatility of instantaneous volatility ξ	75
A.30 Heston model - Hedge European call option with $\mu = 0.1$, $\lambda = 5$ and different volatility of instantaneous volatility ξ . The graphs are shown with respect to changes in time.	76
A.31 Heston model - Hedge European call option with $\mu = 0.3$, $\lambda = 5$ and different volatility of instantaneous volatility ξ . The graphs are shown with respect to changes in time.	77
A.32 Heston model - Hedge European call option with $\mu = 0.6$, $\lambda = 5$ and different volatility of instantaneous volatility ξ . The graphs are shown with respect to changes in time.	78
A.33 Heston model - Hedge European call option with $\mu = 0.1$, $\lambda = 5$ and different positive volatility of instantaneous volatility ξ	79
A.34 Heston model - Hedge European call option with $\mu = 0.1$, $\lambda = 5$ and different negative volatility of instantaneous volatility ξ	80
A.35 Heston model - Hedge European call option with $\mu = 0.3$, $\lambda = 5$ and different positive volatility of instantaneous volatility ξ	81
A.36 Heston model - Hedge European call option with $\mu = 0.3$, $\lambda = 5$ and different negative volatility of instantaneous volatility ξ	82

A.37 Heston model - Hedge European call option with $\mu = 0.6$, $\lambda = 5$ and different positive volatility of instantaneous volatility ξ	83
A.38 Heston model - Hedge European call option with $\mu = 0.6$, $\lambda = 5$ and different negative volatility of instantaneous volatility ξ	84

List of Tables

3.1	Common One-dimensional activation functions and their properties . . .	20
5.1	Few fragments of the trained reweighted measure for the path gains the highest profit and loss.	52

Chapter 1

Introduction

Machine learning has been applied to pricing and hedging derivatives in the financial industry. Thanks to the revolution of electronic trading which makes a large amount of trading data available via the methodical collection of data done by market makers, bankers or their acquisition from data providers, etc. In addition, Kahneman [13] detects that a machine-based decision reduces the emotional bias and results rational and systematic investment choices. Hedging using machine learning has been attractive in recent years and caused various researches.

In an ideally adapted market with frictions, a trader could do hedging using trivial mathematical deduction based on the pricing models. For instance, in the perfect Black-Scholes model, a unique option pricing solution can be obtained from underlying asset prices with a changed measure based on the Radon-Nikodym theorem and a trading portfolio allocation can be calculated by a simple Black-Scholes delta function.

In real markets, prices are normally not adapted and there exist many frictions and uncertainties such as transaction costs, incur costs, liquidity constraints, market impacts, various signals, etc. These factors are added and adjusted in financial models for real trading based on different researchers' knowledge, purpose and preference, which might influence the accuracy and efficiency of derivative hedging and option pricing outcomes. According to the discovery of Kahneman [13], hedging and pricing using machine learning seem to be a reasonable solution.

Many pieces of research relating to machine learning in the financial industry have been done in recent years. These papers structured some usages using different kinds of deep learning strategies. *Kohonen's self-organizing maps (SOMs)*, a method of machine learning, was studied by Huber [12] on the application of hedge funds selection for stable portfolio performance by avoiding concentrations. Benhamou et al. [3] created one type of machine learning called *deep reinforcement learning (DRL)* based on the convolutional neural network, which is widely used for image recognition. He created it for an asset manager to plan the optimal-timing allocation decision for her/his hedging strategies with given market information such as additional contextual information, i.e., financial data, which is other than asset prices and is assumed to have some indirect link with the portfolio assets prediction. One year later, Wu et al. [21] used the same neural network to forecast the financial

market but encode time series to *Gramian angular fields (GAF)* images for the classification task.

In this paper, we use *deep hedging* which was originally devised by the researchers at JP Morgan and ETH Zurich in 2017. Deep hedging is a hedging methodology based on unsupervised deep learning that can be used to hedge options or other derivatives. Multiple frictions such as transaction costs are considered to make this approach more accessible to reality. The hedging strategy is represented by a single feedforward neural network and trained the price data ignoring the existence of statistical arbitrages. Buehler et al. [7] suggest that it is efficient to replace traditional loss functions by an exponential utility function during option pricing. As to preclude the deep hedging strategy from longing underlying assets only, which is caused by the rapid-shifted asset path, there exists a solution that reweights measure and eliminates statistical arbitrages before hedging [8].

Outline

The rest of this paper is organised as follows. In Chapter 2, some characteristics of numerical pricing models, i.e., the Black-Scholes model and the Heston model, are introduced. Chapter 3 describes the structure and features of our unsupervised neural network, feedforward neural network. The buildups and relative methodology for deep hedging are explained in Chapter 4. The numerical results part, Chapter 5, shows the outcomes of deep hedging strategy and reweight measure in several situations. Finally, Chapter 6 is the conclusion summary and further improvements.

Chapter 2

Pricing models

Before introducing my trained deep hedging method, let me give an explanation on two widely used mathematics models, i.e., the Black-Scholes model and the Heston Model. The setups, relative theories and characteristics of both models are the foundations of my deep hedging method.

2.1 Black-Scholes Model

In the simplest form of the Black-Scholes model, we only involve two underlying assets, a riskless asset called cash bond and a risky asset called stock under a physical measurement \mathbb{P} . The cash bond price, B_t , is assumed to increase depending on a certain amount of interest rate as r , which we called the riskless interest rate. The differential equation followed by the cash bond is written as

$$\frac{dB_t}{dt} = rB_t$$

and its unique solution is

$$B_t = B_0 \exp\left(\int_0^t r du\right) = B_0 \exp(rt)$$

The stock with a share price S_t at time t satisfies a stochastic differential equation (SDE), derived via Ito's lemma, in the form of

$$dS_t = \mu_t S_t dt + \sigma S_t dW_t$$

and it can be found that the SDE has a unique solution by solving explicitly

$$S_t = S_0 \exp\left(\left(\mu - \frac{\sigma^2}{2}\right)t + \sigma W_t\right) \quad (2.1.1)$$

where μ is the drift coefficient term; σ is the volatility of the asset, which represent the size of random fluctuations of the asset stock price; W_t is a stochastic variable (Brownian motion) value at time t .

To secure the object is a martingale, the discounted asset price S_t^* is introduced under a risk-neutral probability \mathbb{P}^* [19] as

$$S_t^* := \frac{S_t}{B_t} = \frac{S_0}{B_0} \exp\left(\left((\mu - r) - \frac{\sigma^2}{2}\right)t + \sigma W_t\right)$$

By applying the Ito's formula, one can get

$$dS_t^* = (\mu - r)S_t^* dt + \sigma S_t^* dW_t \quad (2.1.2)$$

Note that in the equation (2.1.2) mentioned above, μ should be equalled to r for martingale which requires the drift term, $\mu - r$, is necessary to be 0 [14]. However, the equation still holds even when the drift coefficient term has a different value with the riskless interest rate. Because if $\mu \neq r$, the investor will demand a premium for holding the stocks. Thus it generally appears while investors are doing trading or hedging [9].

2.1.1 Black-Scholes European Option Pricing

The initial equation for the Black-Scholes Merton (BSM) model was introduced by Black and Scholes in 1973 [4]. It is a differential equation used to calculate the theoretical price of options utilizing five inputs: current stock (or underlying) price, the option's strike price, expected interest rates, time to maturity and expected volatility.

Here, the option is specified as European one and can only be exercised at its expiration as a self-financing investment, with no dividend is paid out before the expiration of the option.

A European call option price $C_t(S_0, K)$ with maturity $t > 0$ and strike $K > 0$ pays at maturity $(S_t - K)^+ = \max(S_t - K, 0)$ and a European put option price $P_t(S_0, K)$ pays at maturity $(K - S_t)^+ = \max(K - S_t, 0)$. The mathematical expressions given by MacBeth and Merville [16] are as below:

$$C_t = S_t N(d_1) - K e^{-r\tau} N(d_2) \quad (2.1.3)$$

and

$$\begin{aligned} P_t &= K e^{-r\tau} - S_t + C \\ &= K e^{-r\tau} N(-d_2) - S_t N(-d_1) \end{aligned} \quad (2.1.4)$$

with

$$d_1 = \frac{\ln\left(\frac{S_t}{K}\right) + \left(r + \frac{\sigma^2}{2}\right)\tau}{\sigma\sqrt{\tau}} \quad \text{and} \quad d_2 = d_1 - \sigma\sqrt{\tau}$$

where τ is the time to expiration, valued as $\tau = T - t$; N is a normal distribution function.

2.1.2 Girsanov's Theorem

As discussed in the previous section, it is clear that the discounted asset price S_t^* is risk-neutral as well as a \mathbb{P}^* -measurable martingale only if when the drift coefficient term μ is equal to the riskless interest rate r . This achievement can only be reached for asset prices in pure mathematical models. In reality, μ can rarely equal to the riskless interest rate as the asset price changes randomly and always contains arbitrages.

To make the unadapted discounted asset price S_t^* suitable for mathematicians to study and do pricing, S_t^* should be re-weighted and becomes a martingale under a new measure, \mathbb{Q} . A well-known theorem, the Girsanov Theorem, is defined to do the measure reweighting on \mathbb{P}^* .

Some additional conditions are assumed before the start of the conduction of the Girsanov Theorem

$$\begin{cases} B_0 = 1 \\ r = 0 \\ \mu \neq r \end{cases}$$

It leads to: the price of cash bond, B_t , will never change with respect to time t and always equal to its initial price B_0 , which is 1; the discounted asset price, S_t^* , has the same value as the share price, S_t , as the effect from the bond price can be neglected under our setting. It also means that the distribution of measure \mathbb{P}^* is the same as the one of physical measure, \mathbb{P} , at the same time.

Then the Black-Scholes Model has the stock price formula and SDE as

$$\begin{cases} S_t^* = S_t = S_0 \exp\left(\left(\mu - \frac{\sigma^2}{2}\right)t + \sigma W_t\right) \\ dS_t^* = dS_t = \mu S_t dt + \sigma S_t dW_t \end{cases} \quad (2.1.5)$$

Theorem 2.1.1 (Girsanov's theorem). *Let W_t be a Brownian motion on $(\Omega, \mathcal{F}, \mathbb{P})$ and $\{\mathcal{F}_t^W\}$ be the natural filtration generated by W_t .*

If $\mathbb{P} \sim \mathbb{Q}$ are two probability measures on \mathcal{F} , then there exists a \mathcal{F}^W -predictable process C such that the probability \mathbb{Q} is defined via the Radon-Nikodym density in the form of

$$\rho_t := \frac{d\mathbb{Q}}{d\mathbb{P}} \Big|_{\mathcal{F}_t} = \exp\left(\int_0^t C_u \cdot dW_u - \frac{1}{2} \int_0^t |C_u|^2 du\right) \quad (2.1.6)$$

Conversely, for fixed $T > 0$ suppose ρ is a strictly positive continuous \mathbb{P} -martingale with $\mathbb{E}_{\mathbb{P}}[\rho_T] = 1$. Then ρ has the representation of (2.1.6) for $t \leq T$ and it defines a measure \mathbb{Q} which is equivalent to \mathbb{P} on $\{\mathcal{F}_t^W : t \leq T\}$. In both cases,

$$\tilde{W}_t := W_t - \int_0^t C_u du \quad (2.1.7)$$

is a \mathbb{Q} Brownian motion.[1]

According to the Girsanov's theorem, SDE of (2.1.7) can be computed in the form of

$$d\tilde{W}_t = dW_t - C_t dt$$

with the solution under \mathbb{Q}

$$\tilde{W}_t = W_t - C_t t \quad (2.1.8)$$

this is equivalent to $dW_t = d\tilde{W}_t + C_t dt$ by changing the orders. Once implement it back into the equation (2.1.5), the represent equation for S_t transforms

$$\begin{aligned} dS_t &= \mu S_t dt + \sigma S_t \left(d\tilde{W}_t + C_t dt \right) \\ &= S_t \left(\mu dt + \sigma d\tilde{W}_t + \sigma C_t dt \right) \\ &= S_t \left((\mu + \sigma C_t) dt + \sigma d\tilde{W}_t \right) \end{aligned} \tag{2.1.9}$$

For making the drift term of the stock price S_t in the above SDE vanishes (i.e., $\mu + \sigma C_t = 0$), there is only one choice for C_t to be taken, which is

$$C_t = -\frac{\mu}{\sigma}$$

Under this value of C_t , the RHS of equation (2.1.9) is a true martingale risk-neutral measure \mathbb{Q} by the Novikov's condition while the Radon-Nikodym derivative, equation (2.1.6), is valid.

The SDE of the stock price becomes

$$dS_t = \sigma S_t d\tilde{W}_t$$

and has a result

$$S = S_0 \exp \left(\sigma \tilde{W}_t - \frac{\sigma^2}{2} t \right)$$

which is a true martingale under the unique probability measure \mathbb{Q} due to the uniqueness of solvable result for C_t .

With holding the value of C_t as $-\frac{\mu}{\sigma}$, the exact expression of Radon-Nikodym derivative (2.1.6) for measure \mathbb{Q} can then be generated as

$$\begin{aligned} \left. \frac{d\mathbb{Q}}{d\mathbb{P}} \right|_{\mathcal{F}_t} &= \exp \left(\int_0^t \left(-\frac{\mu}{\sigma} \right) \cdot dW_u - \frac{1}{2} \int_0^t \left(-\frac{\mu}{\sigma} \right)^2 du \right) \\ &= \exp \left(-\frac{\mu}{\sigma} \cdot W_t - \frac{1}{2} \left(-\frac{\mu}{\sigma} \right)^2 t \right) \\ &= \exp \left(-\frac{\mu}{\sigma} \cdot W_t - \frac{\mu^2}{2\sigma^2} t \right) \end{aligned} \tag{2.1.10}$$

Note that this result can be rechecked by multiplying the asset price before re-weighted, S_t , and the generated Radon-Nikodym derivative formula. According to the characteristic of a true martingale, the conditional expected value of the next observation is equal to its current observation. If all the conditional probabilities for the past observations are given, one can duplicate all the paths and also their initial value. Hence, if the multiplication approaches the initial value of the asset price, then it is a true martingale under the risk-neutral measure \mathbb{Q} .

2.1.3 Delta Hedging

Delta Hedging is an option trading strategy. It can be used to hedge, or reduce, the direct risk which relates to the price shifts of the underlying asset, such as the stock

prices. Financiers often use this approach to offset the risk of holding another single option or the risk of holding an entire portfolio by options that currently exist. The investors tend to enable their hedging strategy to reach a delta neutral state, instead of having any directional bias.

Let's prove the reducing direct risk characteristic of delta hedging. By simplify equation (2.1.1), the underlying asset, $S(t)$, under Black-Scholes model can be represented as

$$dS = \mu S dt + \sigma S dW_t \quad (2.1.11)$$

Set the value of option, $V(S, t)$, depends on the underlying asset and by Ito's formula one will have

$$\begin{aligned} dV &= \frac{\partial V}{\partial t} dt + \frac{\partial V}{\partial S} dS + \frac{1}{2} \frac{\partial^2 V}{\partial S^2} dS^2 \\ &= \frac{\partial V}{\partial t} dt + \frac{\partial V}{\partial S} (\mu S dt + \sigma S dW_t) + \frac{1}{2} \frac{\partial^2 V}{\partial S^2} \sigma^2 S^2 dt \\ &= \left(\frac{\partial V}{\partial t} + \mu S \frac{\partial V}{\partial S} + \frac{1}{2} \sigma^2 S^2 \frac{\partial^2 V}{\partial S^2} \right) dt + \sigma S \frac{\partial V}{\partial S} dW_t \end{aligned} \quad (2.1.12)$$

where $\frac{\partial V}{\partial t} + \mu S \frac{\partial V}{\partial S} + \frac{1}{2} \sigma^2 S^2 \frac{\partial^2 V}{\partial S^2}$ is the drift term of dV and $\sigma S \frac{\partial V}{\partial S}$ is the stochastic term of dV .

In a delta hedged portfolio, Π , investors hedge by long one unit of option and short Δ units of underlying asset price.

$$\Pi = V - \Delta S \quad (2.1.13)$$

By implementing equation (2.1.11) and (2.1.12) into equation (2.1.13), ones can get

$$\begin{aligned} d\Pi &= dV - \Delta dS \\ &= \left(\left(\frac{\partial V}{\partial t} + \mu S \frac{\partial V}{\partial S} + \frac{1}{2} \sigma^2 S^2 \frac{\partial^2 V}{\partial S^2} \right) dt + \sigma S \frac{\partial V}{\partial S} dW_t \right) - \Delta (\mu S dt + \sigma S dW_t) \\ &= \left(\frac{\partial V}{\partial t} + \mu S \frac{\partial V}{\partial S} + \frac{1}{2} \sigma^2 S^2 \frac{\partial^2 V}{\partial S^2} - \Delta \mu S \right) dt + \left(\sigma S \frac{\partial V}{\partial S} - \Delta \sigma S \right) dW_t \end{aligned} \quad (2.1.14)$$

The aim of delta hedging is to reduce the direct risk. Therefore, the stochastic term of $d\Pi$ should approaches zero. We have

$$\sigma S \frac{\partial V}{\partial S} - \Delta \sigma S = 0$$

intuitively, one has the solution as

$$\Delta = \frac{\partial V}{\partial S} \quad (2.1.15)$$

Hence, if the investors have a portfolio strategy of holding one unit of option and $\frac{\partial V}{\partial S}$ units of the underlying asset, they can hedge their risk.

Remark 2.1.2. Combining with equation (2.1.3), (2.1.4) and (2.1.15), it is intuitive that the mathematical expression of delta for Call option pricing, which will be used later, is

$$\Delta_{C_t} = N(d_1) \quad (2.1.16)$$

and for Put option

$$\Delta_{P_t} = -N(-d_1)$$

In other words, the delta hedging under the Black-Scholes model makes the instantaneous net value of short sale to be zero according to the principle of no-arbitrage [11]. The model is self-financing, which means that the values of inflows and outflows of cash are fixed while the time of hedging strategy is operating.

Note that, as the portfolio is self-financing and perfectly hedged, the investor shall gain a return under a risk-free interest rate after some time period t . The portfolio value with no-arbitrage has movements also follow below formula

$$d\Pi = r\Pi dt$$

Implementing the equation (2.1.15) back to (2.1.13) and (2.1.14), one can conduct

$$\begin{aligned} r(V - \Delta S)dt &= \left(\frac{\partial V}{\partial t} + \mu S \frac{\partial V}{\partial S} + \frac{1}{2} \sigma^2 S^2 \frac{\partial^2 V}{\partial S^2} - \Delta \mu S \right) dt \\ &\quad + \left(\sigma S \frac{\partial V}{\partial S} - \Delta \sigma S \right) dW_t \\ r \left(V - \frac{\partial V}{\partial S} S \right) dt &= \left(\frac{\partial V}{\partial t} + \mu S \frac{\partial V}{\partial S} + \frac{1}{2} \sigma^2 S^2 \frac{\partial^2 V}{\partial S^2} - \frac{\partial V}{\partial S} \mu S \right) dt \\ &\quad + \left(\sigma S \frac{\partial V}{\partial S} - \frac{\partial V}{\partial S} \sigma S \right) dW_t \\ r \left(V - S \frac{\partial V}{\partial S} \right) dt &= \left(\frac{\partial V}{\partial t} + \frac{1}{2} \sigma^2 S^2 \frac{\partial^2 V}{\partial S^2} \right) dt \\ rV - rS \frac{\partial V}{\partial S} &= \frac{\partial V}{\partial t} + \frac{1}{2} \sigma^2 S^2 \frac{\partial^2 V}{\partial S^2} \end{aligned}$$

It can eventually turn out to be the PDE of a European call or put under the Black-Scholes model, called the Black-Scholes equation.

$$\frac{\partial V}{\partial t} + \frac{1}{2} \sigma^2 S^2 \frac{\partial^2 V}{\partial S^2} + rS \frac{\partial V}{\partial S} - rV = 0$$

2.2 Heston Model

The Heston model is a popular financial model nowadays for pricing options using stochastic volatility. In the Heston model, the volatility of an asset is assumed to vary stochastically over time, instead of as a constant in the Black-Scholes model. The Heston model is a type of volatility smile model. The volatility smile is a graphical representation of several options with the same expiration dates. The name of smile models comes from the concave shape of the volatility graph, which is similar to a smile.

In Heston model, the stock price, or the underlying price, under risk-neutral measure \mathbb{Q} has the following dynamics

$$dS_t = \mu S_t dt + S_t \sqrt{V_t} dW_t^S, \quad S_0 > 0 \quad (2.2.1)$$

and the variance process V_t is also stochastic with SDE in form of

$$dV_t = \kappa(\theta - V_t)dt + \xi \sqrt{V_t} dW_t^V, \quad V_0 \geq 0 \quad (2.2.2)$$

where μ is the drift coefficient term; V_0 is the initial variance level and has the value of $V_0 = \sigma_0^2$; θ is the long-term average variance level of the price (i.e., the expected value of variance process, V_t , tends to θ as time tends to infinity); κ is the mean reversion speed of variance; ξ is the volatility of instantaneous variance; ρ is the correlation between of the two continuous random walks.

Note that W_t^S, W_t^V are two correlated Brownian motions with correlation ρ under measure \mathbb{Q} , such that $dW_t^S dW_t^V = \rho dt$. The covariance matrix is presented as

$$\text{covariance for } W_t^S \text{ and } W_t^V = \begin{bmatrix} 1 & \rho \\ \rho & 1 \end{bmatrix} \quad (2.2.3)$$

The variance process, V_t is guaranteed to be strictly positive in the Heston model if the Feller condition $2\kappa\theta > \xi^2$ is satisfied.

2.2.1 Characteristic Function

Normally, the stock prices is generated under the Heston model using its unique characteristic function, which describes the probability density function of the model. The characteristic function for the Heston model was first introduced by Heston [10] as part of his seminal paper. For clarifying, we use the numerically robust function illustrated by Broodryk [6].

From equation (2.2.1) and (2.2.2), it is intuitive that the Heston model is parameterised by $(V_0, r, \nu, \lambda, \theta, \rho)$ under the risk-neutral measure \mathbb{Q} . By assuming the log stock price, s_T , under the measure \mathbb{Q} as $s_T = \log(S_T)$, the characteristic function for the Heston model $\phi_{s_T}(u) = \mathbb{E}[e^{i u s_T} | \mathcal{F}_t]$ can then be represented as

$$\phi_{s_T}(u) = \exp(C + DV_t + i u \log(S_t))$$

where

$$C = rTiu + \theta\lambda \left(Tx_- - \frac{1}{a} \log \left(\frac{1 - ge^{-Td}}{1 - g} \right) \right)$$

$$D = \frac{1 - e^{-Td}}{1 - ge^{-Td}} x_-$$

with

$$a = \frac{\nu^2}{2}, \quad b = \lambda - \rho\nu i\mu, \quad c = -\frac{\mu^2 + i\mu}{2}, \quad d = \sqrt{b^2 - 4ac},$$

$$x_{\pm} = \frac{b \pm d}{2a} \quad \text{and} \quad g = \frac{x_-}{x_+}.$$

Note that if we assume $r = 0$, the first term of C will be removed and simplify the equation.

2.2.2 Unreliable Delta Hedging

As derived before, the greek delta in the form of (2.1.14), $\Delta = \frac{\partial V}{\partial S}$. In the Heston model, one can find the representative formula of delta via some mathematical derivations.

However, the Heston model is incomplete in which prices are uniquely determined but is usually not available for perfect hedges. It implies that the delta hedge in the Heston model will not work as perfectly as it was in the Black-Scholes model. Also, Branger and Schlag [5] have attempted to measure the size of tracking error for option hedging under a discrete-time stochastic volatility model. They found that the discreteness error that occurred in the Heston model cannot be improved by a delta hedging approach.

As the deep hedging method under the Heston model used later is under a discrete market, the approach of delta hedge can not be considered as a reliable numerical method. Therefore, we will not have numerical results for comparison when the underlying assets are simulated by the Heston model.

Chapter 3

Feedforward Neural Network (FNN)

The neural network is a special architecture applied in deep learning, which is a popular subfield of machine learning. It can be used to solve difficult issues such as image recognition, data classification, voice recognition, etc. By using neural networks, problems, especially with complex formulas, will become easier and more efficient to conduct the results.

3.1 General Construction

In this paper, only one type of neural network will be used to do the unsupervised deep learning, which is the *feedforward neural network (FNN)*. The definition of FNN is written by Pakkanen [18]. It has a construction of alternately affine function and non-linear function.

Definition 3.1.1. Suppose there is a FNN with input dimensions $I \in \mathbb{N}$, output dimensions $O \in \mathbb{N}$, the number of network layers $r \in \mathbb{N}$ and a representing function $f : \mathbb{R}^I \rightarrow \mathbb{R}^O$. The FNN has $r - 1 \in \{0, 1, \dots\}$ hidden layers, where there are $d_i \in \mathbb{N}$ units in the i -th hidden layer for any $i = 1, \dots, r - 1$, and activation functions $\sigma_i : \mathbb{R}^{d_i} \rightarrow \mathbb{R}^{d_i}$, $i = 1, \dots, r$, where $d_0 := I$ and $d_r := O$, if

$$f = \sigma_r \circ L_r \circ \dots \circ \sigma_1 \circ L_1 \quad (3.1.1)$$

where $L_i : \mathbb{R}^{d_{i-1}} \rightarrow \mathbb{R}^{d_i}$, for any $i = 1, \dots, r$, is an affine function

$$L_i(x) := W^i x + b^i, \quad x \in \mathbb{R}^{d_{i-1}}$$

parameterised by weight matrix $W^i = [W_{j,k}^i]_{j=1, \dots, d_i, k=1, \dots, d_{i-1}} \in \mathbb{R}^{d_i \times d_{i-1}}$ and bias vector $b^i = (b_1^i, \dots, b_{d_i}^i) \in \mathbb{R}^{d_i}$. We shall denote the class of such functions f by

$$f \in \mathcal{N}_r(I, d_1, \dots, d_{r-1}, O; \sigma_1, \dots, \sigma_r) \quad (3.1.2)$$

If $\sigma_i(x) = (g(x_1), \dots, g(x_{d_i}))$, $x = (x_1, \dots, x_{d_i}) \in \mathbb{R}^{d_i}$, for some $g : \mathbb{R} \rightarrow \mathbb{R}$, we write g in place of σ_i in equation 3.1.1 and 3.1.2.

The integers r, d_1, \dots, d_{r-1} are called the hyperparameters of the FNN. The weights in W^1, \dots, W^r and biases in b^1, \dots, b^r are called the actual parameters of the network and can be written in a vector $\theta = (W^1, \dots, W^r, b^1, \dots, b^r)$.

3.2 Activation Functions

Unlike affine functions, the activation functions are mostly non-linear. The common affine functions can be divided into two types: one-dimensional and multi-dimensional. In this paper, only the one-dimensional affine functions are discussed. Some key one-dimensional examples are in Table 3.1.

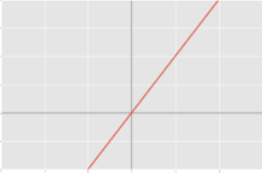
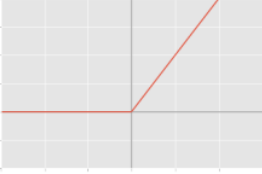
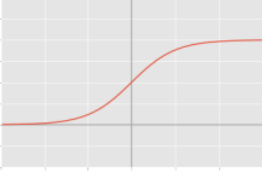
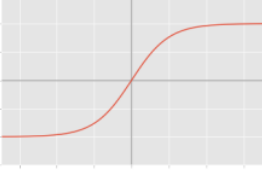
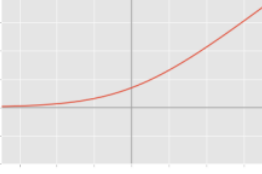

Activation	Definition	Graph	Range
Identity (Id)	$g(x) = x$		\mathbb{R}
Rectified linear unit (ReLU)	$g(x) = \max\{x, 0\}$		$[0, \infty)$
Sigmoid	$g(x) = \frac{1}{1+e^{-x}}$		$(0, 1)$
Hyperbolic tangent (tanh)	$g(x) = \frac{e^x - e^{-x}}{e^x + e^{-x}}$		\mathbb{R}
Softplus	$g(x) = \log(1 + e^x)$		$(0, \infty)$
Gaussian	$g(x) = e^{-x^2}$		$(0, 1]$

Table 3.1: Common One-dimensional activation functions and their properties

The *Identity* is normally used only in the output layer, as it may reduce the resulting neural network into a simple affine function when applying simultaneously in all layers. The *Rectified linear unit (ReLU)* is a common activation function in the hidden layers. Mathematically, *ReLU* only keeps the non-negative values and enables a numerically efficient deduction. Both *Sigmoid* and *Hyperbolic tangent* are saturating. Because the output of *Sigmoid* and *Hyperbolic tangent* are bounded, these two activation functions are popularly used in the output layer for making the neural network result bounded in a controllable range. The *Softplus* is the smooth function of *ReLU* for some specific situations.

3.3 Loss Functions

Suppose we observe $N \in \mathbb{N}$ samples of input variables X with input dimension $I \in \mathbb{N} (= \{1, 2, \dots, \})$,

$$\begin{matrix} x_1^1 & \dots & x_I^1 \\ \vdots & & \vdots \\ x_1^N & \dots & x_I^N \end{matrix}$$

and matching N samples of \mathbb{R} -valued reference value Y ,

$$\begin{matrix} y^1 \\ \vdots \\ y^N \end{matrix}$$

A function $\ell : \mathbb{R}^O \times \mathbb{R}^O \rightarrow \mathbb{R}$ is called loss function and the realised loss is computed as

$$\ell(f(X), Y)$$

where $f : \mathbb{R}^I \rightarrow \mathbb{R}^O$, $f \in \mathcal{N}_r(I, d_1, \dots, d_{r-1}, O; \sigma_1, \dots, \sigma_r)$, is the neural network. Theoretically, for X and Y random and joint, f can be sought till optimal by minimising risk

$$\mathbf{E}[\ell(f(X), Y)] \tag{3.3.1}$$

However, the distribution of X and Y are typically unknown in practice. The risk is required to be computed, equation (3.3.1), as an empirical risk via the average loss

$$L(f) := \frac{1}{N} \sum_{i=1}^N \ell(f(X^i), Y^i)$$

The average loss of the whole X and Y set does not operate efficiently for large N . The idea of minibatch, B , is introduced as a random subset of samples with a given size

$$B \subset \{1, \dots, N\}$$

Therefore, it is reasonable to approach the result by minimising the average loss of different minibatches over and over. One pass of the neural network training process over each minibatches' training data constitutes a training epoch. The minibatch risk is defined as

$$L(f_\theta) := \frac{1}{\#B} \sum_{i \in B} \ell(f_\theta(X^i), Y^i)$$

where the neural network $f_\theta = f$ is then fully determined by the parameter vector θ which need to be optimized.

Chapter 4

Pricing and Hedging by Unsupervised Deep Learning

Buehler et al. [7] has introduced a neural network that can hedge a portfolio of derivatives, or underlying assets, in the presence of transaction costs in a financial market. In this section, a similar method will be introduced. For simplicity, the method will be without any market frictions. As it is found in practice that the result of hedging strategy via unsupervised deep learning may occur to be over-hedged, the probability measure of the underlying assets is required to be modified. Buehler et al. [8] have found that the measure reweighting can also be done using deep learning.

4.1 Setting: Discrete Time-market Simulation

Suppose there is a discrete-time financial market with $T \in \mathbb{N}$ finite trading periods (i.e., the maturity can be either considered as T or one, which is T/T) and $N \in \mathbb{N}$ risky (or underlying) assets. The trading assets in each trading period are denoted as

$$S_t := \{S_{t,i}\} = (S_{t,1}, S_{t,2}, \dots, S_{t,N})$$

where $t = 0, 1, \dots, T$ are different time steps and $i = 1, 2, \dots, N$ represent different asset paths. The probability measure for the market is \mathbb{P} , where $\mathbb{P}[\{\omega_i\}] > 0$ for all i . It is assumed that the non-negative stochastic process is adapted over a filtered probability space $(\Omega, (\mathcal{F})_{t=0}^T, \mathbb{P})$. And for a simpler model and calculation, the riskless interest risk, r , takes the value of zero.

The underlying asset price going to be processed is either collected from the real market data or simulated as a random stochastic process according to the SDEs for different financial models. When pre-processing or simulating S_t , the scale for each asset price, $S_{t,i}$, should not be too large, as the training by unsupervised deep learning process may cause a failure.

If the risky asset prices are collected from the real market data, they should be pre-processed into a matrix with the number of time steps in columns and the number of asset paths in rows. For each asset path, the total number of time steps is required to be equal and the existence of missing data cannot be there. The prices can also be

re-scaled by the mean of all the values in the price matrix or by any other numbers with a similar scale.

Two types of financial models are used when doing asset price simulation, the Black-Scholes model and the Heston model. These two types of models have different SDEs but have similar simulation methods.

As mentioned before, the continuous-time Black-Scholes price process has the formula as

$$S_t^{\text{BS}} = S_0 \exp(\mu t + \sigma W_t), \quad t \in [0, 1]$$

When doing the simulation, the stochastic variable W_t is replaced by a sum of some normal (i.e., Gaussian) distributed independent random variables with mean zero and standard derivation $1/T$. These mutually generated Gaussian distributions are adapted as $\zeta_u \sim N(0, \frac{1}{T})$ and have

$$W_t = \sum_{u=1}^t \zeta_u, \quad t \in [0, 1]$$

and the price process is constructed as follow

$$S_t^{\text{BS}} = S_0 \exp\left(\mu \frac{t}{T} + \sigma \sum_{u=1}^t \zeta_u\right), \quad t = 0, 1, \dots, T$$

In the Heston model, there are two standard Brownian motions, dW_t^S and dW_t^V . Two distributions, ζ_t^S and ζ_t^V , are generated for the two stochastic processes using the covariance matrix (2.2.3). The price process is transformed from the Heston SDEs

$$\begin{aligned} dV_t^H &= \kappa(\theta - V_t^H)dt + \xi \sqrt{V_t^H} dW_t^V \\ dS_t^H &= \mu S_t^H dt + S_t^H \sqrt{V_t^H} dW_t^S \end{aligned}$$

into the form of

$$\begin{aligned} V_{t+1}^H &= V_t^H + \kappa(\theta - V_t^H)dt + \xi \sqrt{V_t^H} \zeta_t^V \sqrt{dt} \\ S_{t+1}^H &= S_t^H \exp\left(\left(\mu - \frac{V_t^H}{2}\right)dt + \sqrt{V_t^H} \zeta_t^S \sqrt{dt}\right) \end{aligned} \quad (4.1.1)$$

by taking $dt = 1/T$. The value of underlying asset price at expiry time T is deducted from the initial value of instantaneous volatility and underlying asset price using recursion through time steps.

4.2 Deep Hedging

Define an adapted, self-financing trading strategy as

$$\delta_t = (\delta_{t,1}, \delta_{t,2}, \dots, \delta_{t,d})$$

with $t = 0, 1, \dots, T - 1$. If δ_t is equal to zero, it means that the trader sells everything he holds and only left cash in his account. The costs during trading, such

as transaction cost and incur cost, are all assumed equalling to zero. Then the liquidation wealth of the trading strategy δ at expiry time T is

$$V_T(\delta; S) = \sum_{t=1}^T \delta_{t-1} \cdot (S_t - S_{t-1})$$

Assume now we are the market makers, or the bankers, our hedging strategy aims to hedge a contingent claim Z . This claim has a value $p \in \mathbb{R}$ at time 0. The price p can also be considered as an additional cash flow which is given by the financial market (e.g., a market quote) or by the market maker's pricing and is needed to inject into our portfolio. If p is positive, it means that the market maker has initially sold the claim. If p is negative, it means that the market maker has bought the claim at time 0. The payoff gotten at maturity T by our claim Z is

$$Z_T = f(S_0, \dots, S_T)$$

where $f : \mathbb{R}^{T+1} \rightarrow \mathbb{R}$ is a measurable function.

The profit and loss value if we trade the underlying followed by a portfolio δ which is counteracting the risk brought from Z at time T is

$$\text{P\&L}_{T,Z}(p, \delta; S) = p + V_T(\delta; S) - Z_T$$

According to the risk preferences, the chosen hedging portfolio δ needs to offset the risk brought by claim Z . Hence, the aim of deep hedging is to find the specific portfolio δ which enables the value of $\text{P\&L}_{T,Z}(p, \delta; S)$ to be optimal for each time step t . We define an objective function, i.e., a loss function, $\ell : \mathbb{R} \rightarrow \mathbb{R}$ such that, if we try to minimise the finite value for finding the result of δ we are aiming for

$$\mathbb{E}[\ell(\text{P\&L}_{T,Z}(p, \delta; S))]$$

over all adapted process δ , our hedging strategy will approach optimal.

Remark 4.2.1. For example, the objective function can be deemed as a quadratic loss function

$$\ell(x) := x^2$$

or the utility indifference pricing function

$$\ell(x) := -U(x)$$

with some utility function U , which has a further explanation in Section 4.3.

In reality, it is complex to find out the result of optimal trading strategy δ over all adapted asset paths. Approaches using deep learning may make things simpler and time saving.

Suppose that the trading strategy δ is only based on the asset price and a measurable function $f_t : \mathbb{R}^{t+1} \rightarrow \mathbb{R}$ exists. Such that

$$\delta_t = f_t(S_0, \dots, S_t)$$

over all time periods from 0 to T , i.e., time t takes the value $0, 1, \dots, T$. This function determines the trading strategy as a result and it may resort the FNN as a proxy approach.

Suppose there is a FNN $\phi_t(\cdot; \theta_t)$, which is parameterised by vector θ_t for any $t = 0, \dots, T - 1$. Replace the measurable function f_t by the network ϕ_t

$$\delta_t^{(\theta_t)} = \phi_t(S_0, \dots, S_t; \theta_t)$$

and optimise over the trading strategies. The parameter vector θ_t is trained over epochs and becomes a fixed value when reaching the optimal empirical risk.

In practice, the FNN is unsupervised as finding the numerical result of portfolio strategy is not efficient, typically during trading. However, having a separate network ϕ_t for every $t = 0, \dots, T - 1$ may result too many parameters θ_t if the maturity T is large and may also be inefficient as it neglects the fact that many hedging strategies enjoy some form of continuity in time.

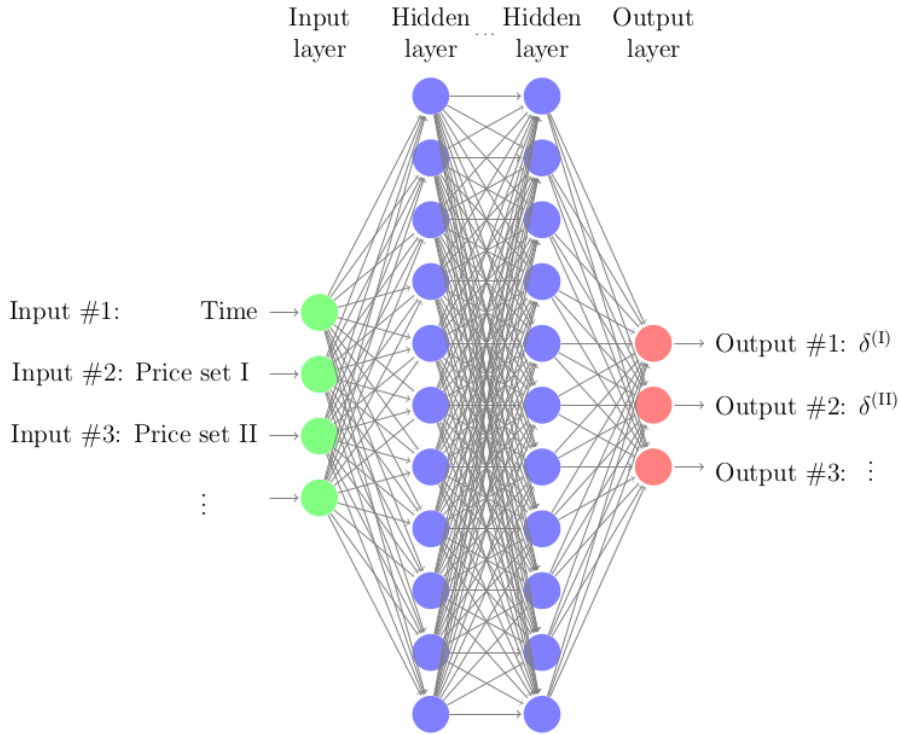


Figure 4.1: The single feedforward neural network (FNN) illustrated by Horvath et al. [2]. Input #1 is the series of time steps t . Input #2, #3, ..., are the sets containing price paths for one asset. FNN here hedges among these assets and results the corresponding hedging strategies.

Horvath et al. [2] has illustrated a more efficient approach if a single feedforward

neural network is used to represent $\phi_0, \dots, \phi_{T-1}$ by taking time and current and lagged asset price as its inputs

$$\delta_t^{(\theta)} = \phi_t(t, S_t, \dots, S_{t-l}; \theta)$$

where $\phi(\cdot; \theta) : \mathbb{R}^{d(l+1)+1} \rightarrow \mathbb{R}^d$ is a FNN and $l = 0, 1, \dots$ determines the size of the lookback window. l can be zero if the asset price is a Markov process and the claim Z is not path-dependent.

4.3 Exponential Utility Indifference Pricing

To further apply the deep hedging methodology on other financial products such as derivatives, it is required to measure the price $p \in \mathbb{R}$ of claim Z during training process. Buehler et al. [7] have pointed out that a method called *utility indifference pricing* can be used as a convenient solution with the combination of deep hedging.

Suppose the loss function ℓ is given by $\ell(x) := -U(x)$ for some utility function $U : \mathbb{R} \rightarrow \mathbb{R}$. Assume that the utility function U is strictly both increasing and concave.

As Buehler et al. [7] have defined in their paper that the indifference price is the amount of cash difference that is charged between selling the claim Z and not doing so. As the optimal value for profit and loss will not change for selling the claim Z or not, then

$$\inf_{\delta} \mathbb{E} [\ell (\text{P\&L}_{T,Z}(p, \delta; S))] = \inf_{\delta} \mathbb{E} [\ell (\text{P\&L}_{T,0}(0, \delta; S))]$$

By implementing the utility function U , we have the LHS

$$\begin{aligned} \inf_{\delta} \mathbb{E} [\ell (\text{P\&L}_{T,Z}(p, \delta; S))] &= \inf_{\delta} \mathbb{E} [-U (\text{P\&L}_{T,Z}(p, \delta; S))] \\ &= \sup_{\delta} \mathbb{E} [U (\text{P\&L}_{T,Z}(p, \delta; S))] \end{aligned}$$

and the RHS

$$\begin{aligned} \inf_{\delta} \mathbb{E} [\ell (\text{P\&L}_{T,0}(0, \delta; S))] &= \inf_{\delta} \mathbb{E} [-U (\text{P\&L}_{T,0}(0, \delta; S))] \\ &= \sup_{\delta} \mathbb{E} [U (\text{P\&L}_{T,0}(0, \delta; S))] \end{aligned}$$

Wherefore, one needs to satisfy

$$\sup_{\delta} \mathbb{E} [U (\text{P\&L}_{T,Z}(p, \delta; S))] = \sup_{\delta} \mathbb{E} [U (\text{P\&L}_{T,0}(0, \delta; S))]$$

Hence, the price p is the *utility indifference price* of claim Z under U if it solves

$$\sup_{\delta} \mathbb{E} \left[U \left(x + \underbrace{p + V(\delta; S) - Z_T}_{=\text{P\&L}_{T,Z}(p, \delta; S)} \right) \right] = \sup_{\delta} \mathbb{E} \left[U \left(x + \underbrace{V(\delta; S)}_{=\text{P\&L}_{T,0}(0, \delta; S)} \right) \right] \quad (4.3.1)$$

where $x \in \mathbb{R}$ is the amount of cash in account at time 0. Because the function $\sup_{\delta} \mathbb{E} [U(\cdot)]$ determines the expected utility level, the influence of x can be neglected

and considered as equal to zero. In other words, market maker has the same expected utility if he sells the claim Z , receives a p amount of cash and trades the underlying assets in the market or he/she holds the claim Z without selling it.

There are many kinds of utility functions for different purposes. The key example of utility function is the exponential utility. It has the expression as

$$U_\lambda(x) = -\exp(-\lambda x)$$

with a risk aversion parameter $\lambda > 0$. In some paper, e.g., [8] and [2], it is written as $U_\lambda(x) = -\frac{1}{\lambda} \exp(-\lambda x)$. The fraction part influence only on utility function U_λ scaling, not its characteristics, and will not change the results of utility indifference price p .

Being simplified, equation (4.3.1) turns to be

$$\begin{aligned} \text{RHS} &= \sup_{\delta} \mathbb{E}[U_\lambda(V(\delta; S))] = \sup_{\delta} \mathbb{E}[U_\lambda(p + V(\delta; S) - Z_T)] = \text{LHS} \\ &= \sup_{\delta} \mathbb{E}[\exp(-\lambda p) \cdot U_\lambda(V(\delta; S) - Z_T)] \\ &= \exp(-\lambda p) \sup_{\delta} \mathbb{E}[U_\lambda(V(\delta; S) - Z_T)], \end{aligned}$$

A unique solution can be solved

$$p = -\frac{1}{\lambda} \log \left(\frac{\sup_{\delta} \mathbb{E}[U_\lambda(V(\delta; S))]}{\sup_{\delta} \mathbb{E}[U_\lambda(V(\delta; S) - Z_T)]} \right)$$

Then, for finding the value of indifference price p , the only thing is to solve the utility level for the profit and loss both with and without position $-Z$. It is much simpler and faster than the traditional method.

Applying deep learning, there would only be two times training to get the results: $\hat{\delta}^0$ trained by the loss function $\ell(\delta; S) = -U_\lambda(V(\delta; S))$ and $\hat{\delta}^Z$ trained by the loss function $\ell(\delta; S) = -U_\lambda(V(\delta; S) - Z_T)$. Finally, by implementing the result of two trading strategy, the price p for claim Z is estimated using the formula

$$\hat{p} = -\frac{1}{\lambda} \log \left(\frac{\frac{1}{N} \sum_{i=1}^N U_\lambda(V(\hat{\delta}_i^0; S_i))}{\frac{1}{N} \sum_{i=1}^N U_\lambda(V(\hat{\delta}_i^Z; S_i) - Z_T)} \right)$$

4.4 Probability Measure Reweighting

Hedging using deep hedging may sometimes cause a result portfolio approaching one especially when the underlying asset market price is shifting monotonously and rapidly. The reason for this is the existence of statistical arbitrage.

Normally, we hedge a derivative with underlying which has higher utility. However, when the market is increasing/decreasing rapid enough, the neural networks may consider that statistical arbitrages are large enough for hedging and prefer to do nothing. Since then, all cash will be used to long or short the the underlying assets

in order to offset the risk. This cannot be said as a mathematical error once future asset's paths are disclosed. But, as the market is moving randomly and long-term unpredictable, hedging the claim by portfolio approximately equal to one is too risky and is not allowed in financial institutions.

Buehler et al. [8] have illustrated a method in their thesis as to reweight the probability of each asset path before it is used to be hedged for the trading strategy δ . With deep learning, the reweighting method enables the change of underlying asset probability measure from the physical one, \mathbb{P} , to a new measure, \mathbb{Q} , which enables assets free from statistical arbitrage. The result of new measure \mathbb{Q} seeks to have the same result as the one of the Radon-Nikodym density, equation (2.1.10), achieves.

Suppose there is a set of underlying assets with N paths and measure \mathbb{P} , the aim is to remove the statistical arbitrage from the set for further hedging process. Suppose further that the loss function for the neural network still holds as $\ell(x) := -U(x)$ for some utility function $U : \mathbb{R} \rightarrow \mathbb{R}$.

The claim price at maturity, Z_T , and the utility indifference price, p , may be neglected because they only relate to the hedging strategy computation when offsetting the statistical arbitrage among underlying assets. The only focused term is the liquidation value term. The measure reweighting method is parametrized by a neural network with outcome δ^* as the liquidation wealth

$$\mathbb{E}[\ell(V(\delta; S))]$$

is optimised. In other words,

$$\begin{aligned} \mathbb{E}[\ell(V(\delta^*; S))] &= \inf_{\delta} \mathbb{E}[\ell(V(\delta; S))] \\ &= \inf_{\delta} \mathbb{E}[-U_{\lambda}(V(\delta; S))] \\ &= \sup_{\delta} \mathbb{E}[U_{\lambda}(V(\delta; S))] \end{aligned}$$

If the result satisfies $\mathbb{E}[-U_{\lambda}(V(\delta^*; S))] > 0$, then the market under new measure \mathbb{Q} is given by

$$\frac{d\mathbb{Q}}{d\mathbb{P}} = \frac{-U_{\lambda}(V(\delta^*; S))}{\mathbb{E}_{\mathbb{P}}[-U_{\lambda}(V(\delta^*; S))]}$$

For real market data, all asset paths initially have the same probability, i.e., measure \mathbb{P} is equally weighted. The new probability weights q^* is generated for each path under the new measure \mathbb{Q} via

$$q^* = \frac{-U_{\lambda}(V(\delta^*; S))}{\sum -U_{\lambda}(V(\delta^*; S))}$$

where the sum refers to the sum of all paths.

Chapter 5

Numerical Results

Suppose a set of asset prices are simulated using the methodology in Section 4.1, and our claim Z is a European call option

$$Z_T = (S_T^{BS} - K)^+$$

with initial cash $x = 0$. The loss function for empirical risk determination is $\ell := U(x)$ where U is the exponential utility function

$$U_\lambda(x) = -\exp(-\lambda x)$$

with a risk aversion parameter $\lambda > 0$.

5.1 Deep Hedging and Measure Reweighting in Black-Scholes Model

In this section, the underlying prices are generated followed by the Black-Scholes price process with fixed parameters:

- Number of market pathes $N = 10^5$
- Number of time periods $T = 100$
- Initial underlying price $S_0 = 1$
- Strike price $K = 1$
- Stochastic volatility $\sigma = 0.5$

The drift coefficient μ and risk aversion parameter λ in utility function are left as variables. According to Section 4.3 and 4.4, the loss function for optimizing deep hedging risk is

$$\begin{aligned}\ell^{DH}(\delta; S) &= \ell(p + V(\delta; S) + Z_T) \\ &= -U_\lambda(p + V(\delta; S) + Z_T) \\ &= \exp(-\lambda \cdot (p + V(\delta; S) + Z_T))\end{aligned}$$

and for measure reweighting risk is:

$$\begin{aligned}\ell^{RW}(\delta; S) &= \ell(V(\delta; S)) \\ &= -U_\lambda(V(\delta; S)) \\ &= \exp(-\lambda \cdot V(\delta; S))\end{aligned}$$

The FNN we used has a structure

$$f \in \mathcal{N}_4(2, 100, 100, 100, 1; \text{ReLU}, \text{ReLU}, \text{ReLU}, \text{tanh})$$

Because the financial intuitions hedge position should be between -1 to 1, the output activation function is helpful to choose as *Hyperbolic tangent*. It can be replaced by *Sigmoid* when shorting is not allowed in the market.

Whether the deep hedging strategy performs well requires to be verified when the market is monotonically increasing or decreasing, i.e., the drift coefficients in the Black-Scholes price process formula is not equal to zero. Its conclusion is the premise for the next section because the results of deep hedging with a measure transformed using the Radon-Nikodym density (will call this measure as *Radon-Nikodym measure* later) and the delta hedging is not reliable in the Heston model and makes the Heston model having no numerical reference. Therefore, by comparing the performance of numerical delta hedging and deep hedging with different measures in the Black-Scholes model, the reliability of different strategies can be identified.

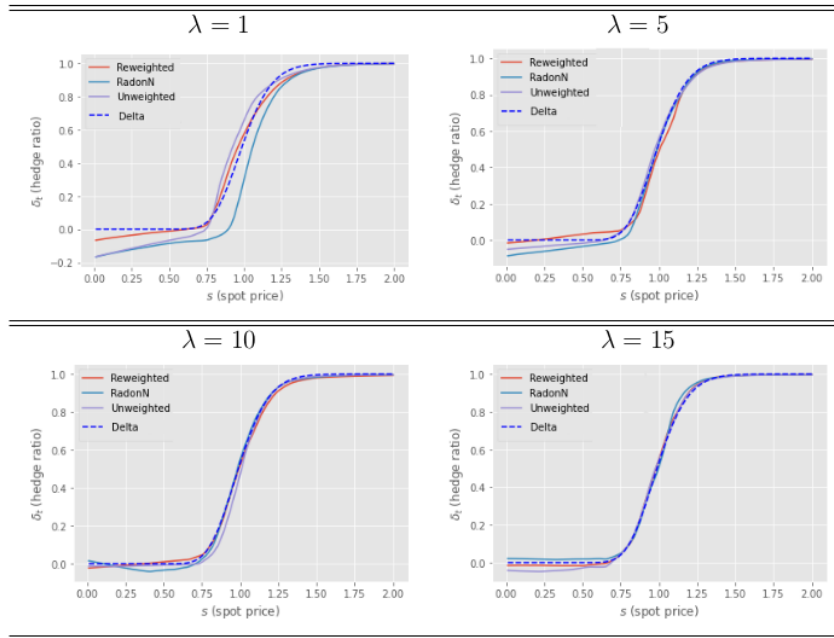


Figure 5.1: Black-Scholes model - Comparison of hedge ratio between deep hedging strategy with reweighted, Radon-Nikodym and unweighted measure and the delta hedging strategy with drift term $\mu = 0$ at time $t/T = 0.9$.

The first step of our detection is to find the best suitable risk aversion λ for the optimal output via deep learning. Both deep hedging strategy and delta hedging strategy are lunched for the measurable underlying assets, i.e., with drift term μ equals to zero, and their results are shown in Figure 5.1. We found that the higher value risk aversion has, the more proper the trained hedging strategies are.

The histogram in Figure 5.2 represents the distribution of profit and loss based on hedging the European call option with adapted underlying assets. The results of different deep hedging strategies are quite similar to the one of the numerical delta hedging strategy. Therefore, deep hedging is an applicable method for portfolio building up. The line graph on the right-hand side of Figure 5.2 is the graph of the hedging strategies for a particular underlying path. The curves indicate that the deep hedging strategies properly match the numerical one with $\mu = 0$ and large λ .

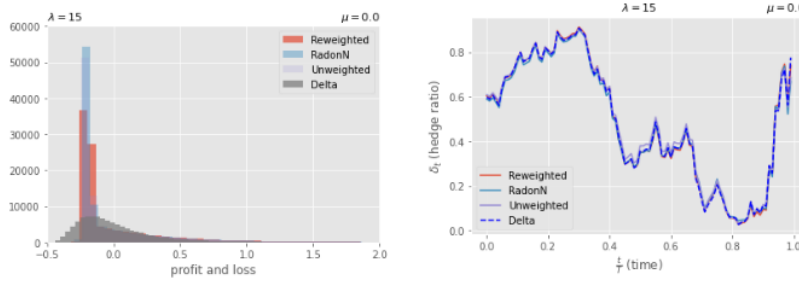


Figure 5.2: Black-Scholes model - The profit and loss histogram for European call option and hedge ratio for a hedge path among deep hedging strategy with reweighted, Radon-Nikodym and unweighted measure and the delta hedging strategy with drift term $\mu = 0$ and risk aversion $\lambda = 15$.

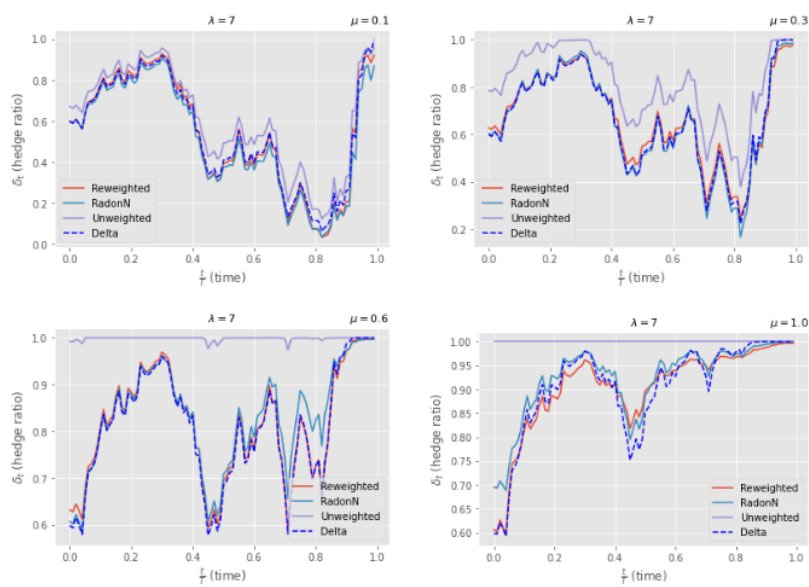


Figure 5.3: Black-Scholes model - Hedge European call option with $\lambda = 7$ for different positive drift term μ . The graphs are shown with respect to changes in time.

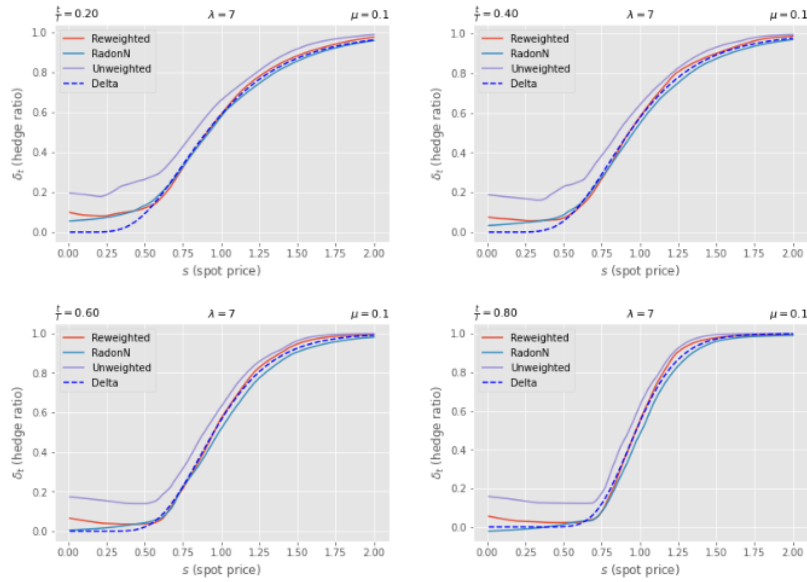


Figure 5.4: Black-Scholes model - Comparison of the hedge ratio between deep hedging strategy with reweighted, Radon-Nikodym and unweighted measure and the delta hedging strategy with $\lambda = 7$ and $\mu = 0.1$

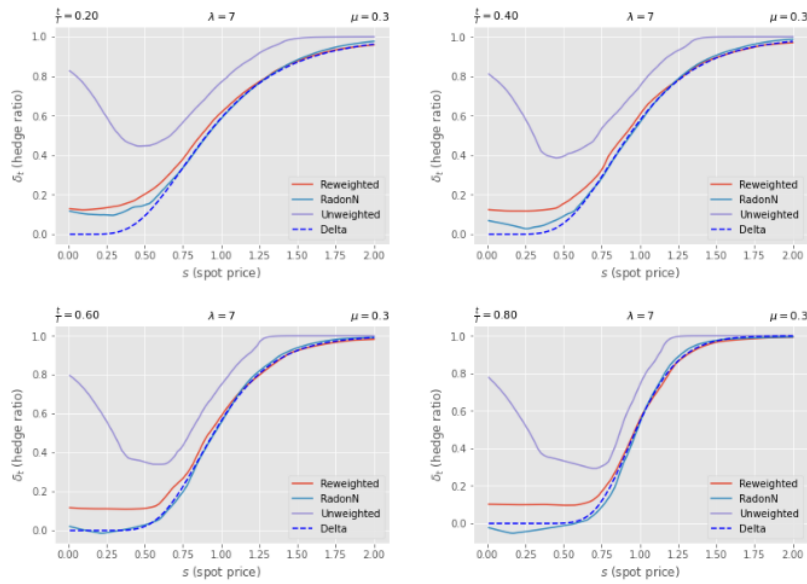


Figure 5.5: Black-Scholes model - Comparison of the hedge ratio between deep hedging strategy with reweighted, Radon-Nikodym and unweighted measure and the delta hedging strategy with $\lambda = 7$ and $\mu = 0.3$.

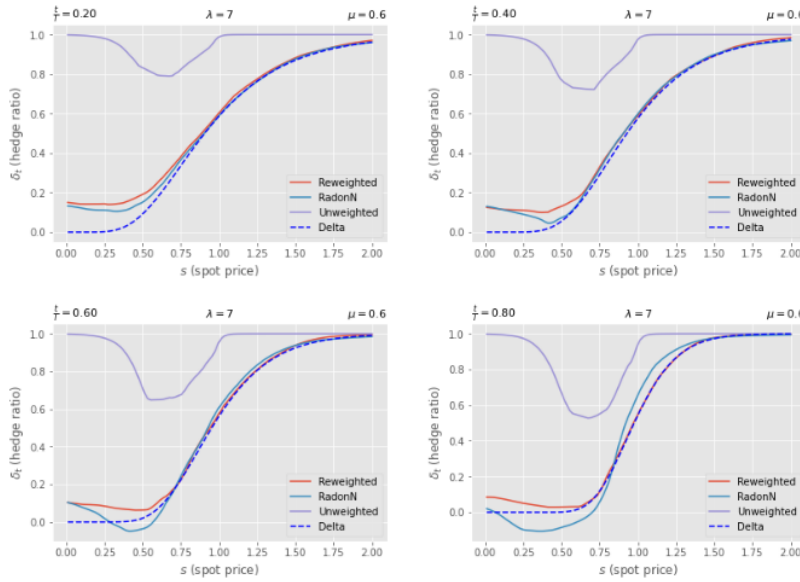


Figure 5.6: Black-Scholes model - Comparison of the hedge ratio between deep hedging strategy with reweighted, Radon-Nikodym and unweighted measure and the delta hedging strategy with $\lambda = 7$ and $\mu = 0.6$.

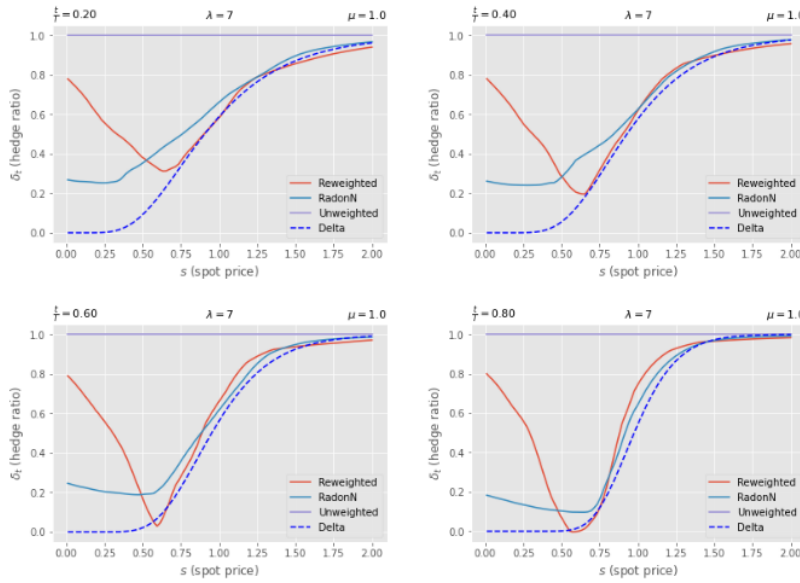


Figure 5.7: Black-Scholes model - Comparison of the hedge ratio between deep hedging strategy with reweighted, Radon-Nikodym and unweighted measure and the delta hedging strategy with $\lambda = 7$ and $\mu = 1.0$.

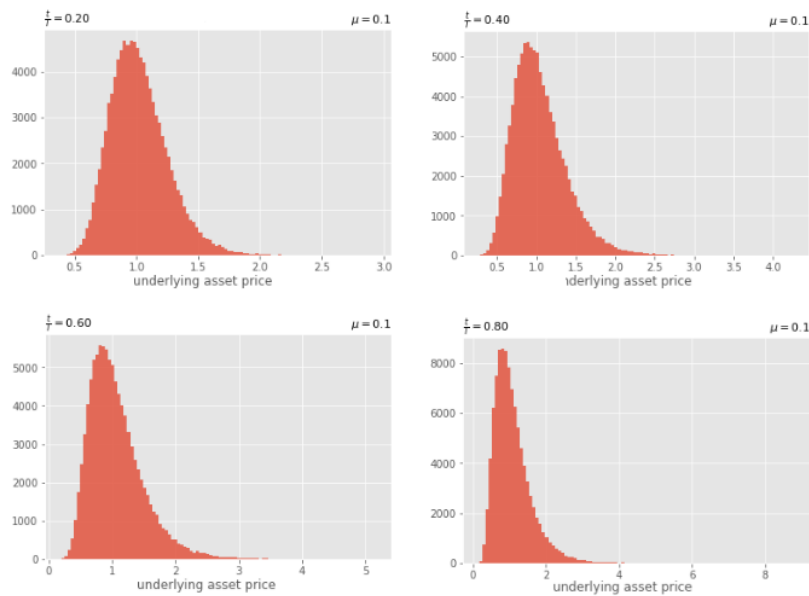


Figure 5.8: Black-Scholes model - The underlying asset price histogram simulated by computer with drift term $\mu = 0.1$.

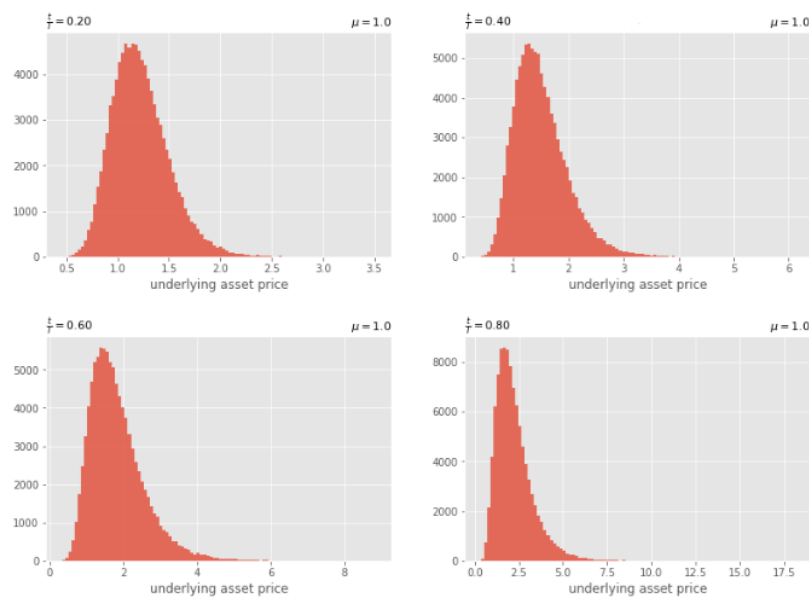


Figure 5.9: Black-Scholes model - The underlying asset price histogram simulated by computer with drift term $\mu = 1$.

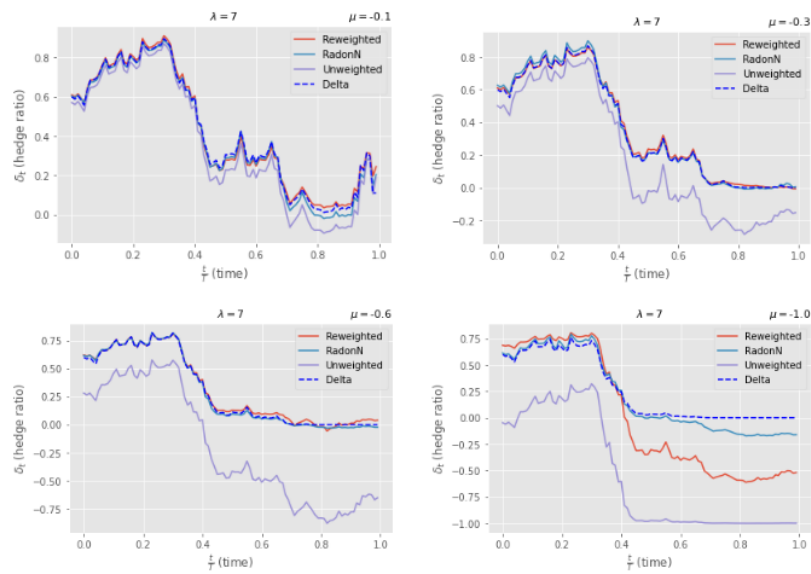


Figure 5.10: Black-Scholes model - Hedge European call option with $\lambda = 7$ for different negative drift term μ . The graphs are shown with respect to changes in time.

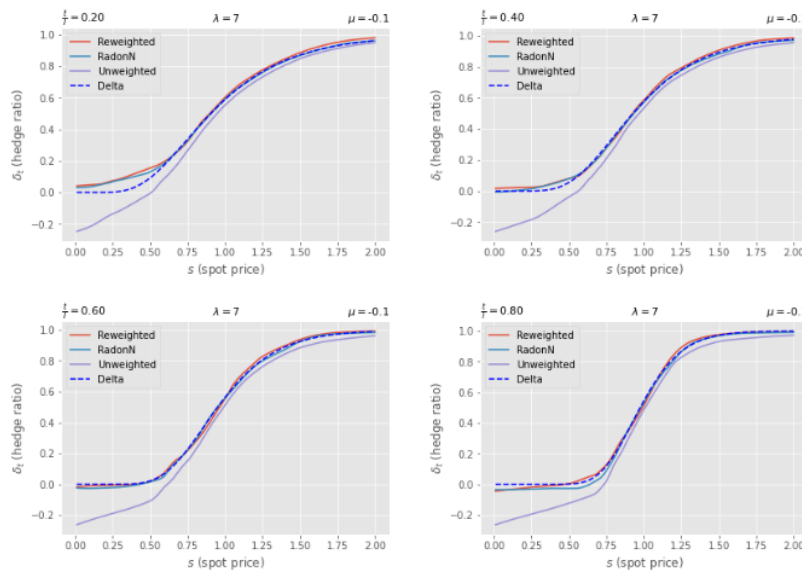


Figure 5.11: Black-Scholes model - Comparison of the hedge ratio between deep hedging strategy with reweighted, Radon-Nikodym and unweighted measure and the delta hedging strategy with $\lambda = 7$ and $\mu = -0.1$.

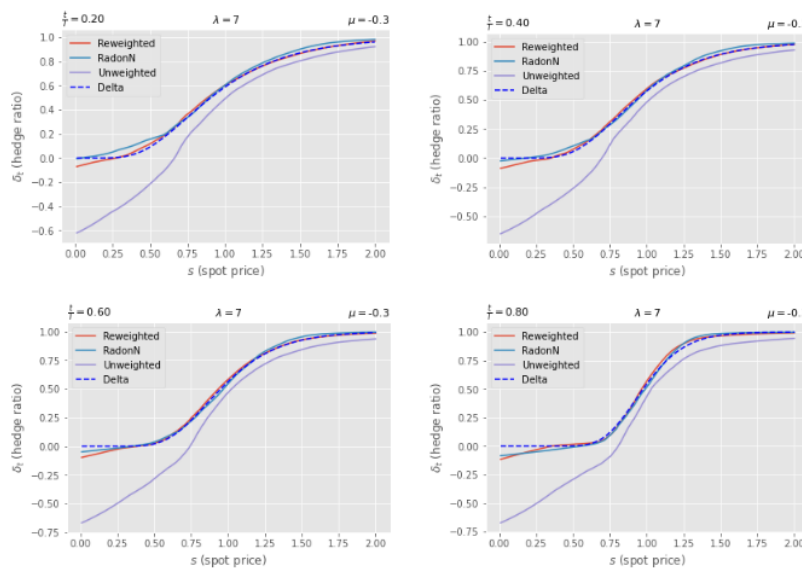


Figure 5.12: Black-Scholes model - Comparison of the hedge ratio between deep hedging strategy with reweighted, Radon-Nikodym and unweighted measure and the delta hedging strategy with $\lambda = 7$ and $\mu = -0.3$.

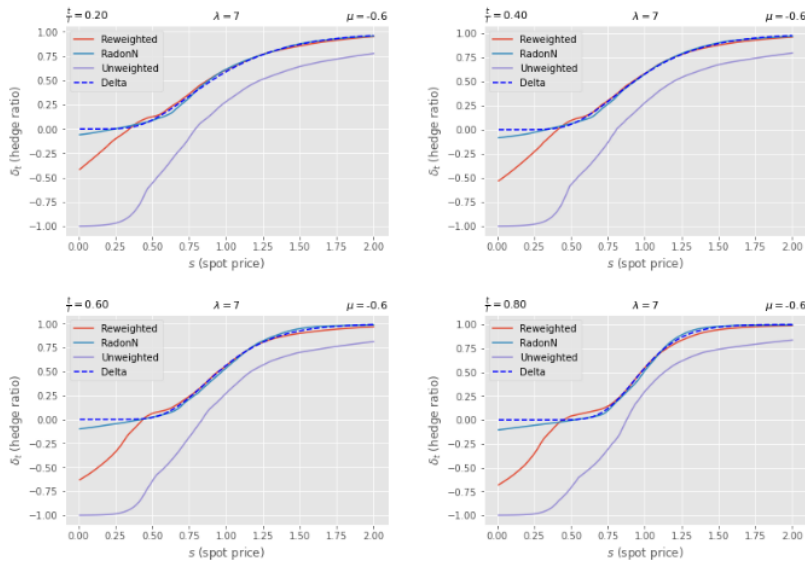


Figure 5.13: Black-Scholes model - Comparison of the hedge ratio between deep hedging strategy with reweighted, Radon-Nikodym and unweighted measure and the delta hedging strategy with $\lambda = 7$ and $\mu = -0.6$.

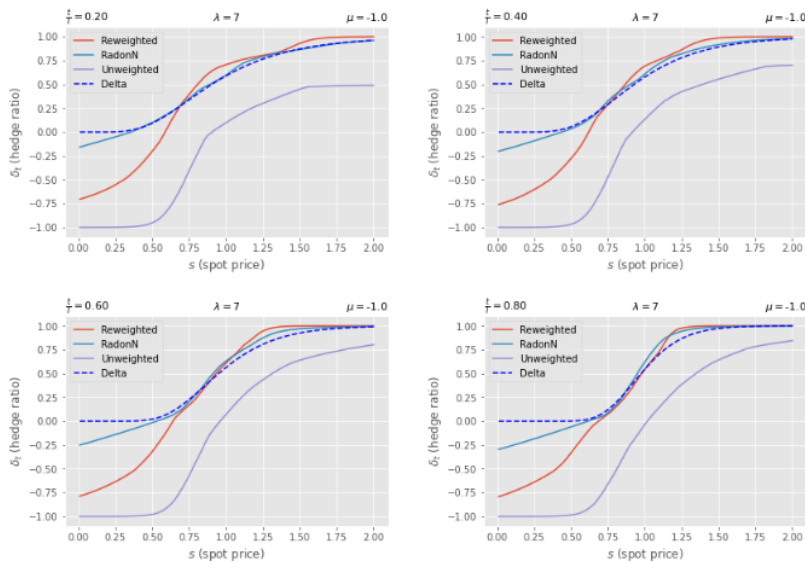


Figure 5.14: Black-Scholes model - Comparison of the hedge ratio between deep hedging strategy with reweighted, Radon-Nikodym and unweighted measure and the delta hedging strategy with $\lambda = 7$ and $\mu = -1.0$.

Figure 5.3 to Figure 5.7 indicates that the trained results from deep hedging with either reweighted measure or the Radon-Nikodym measure match the one from numerical delta hedging. When the drift term is increasing, the results of the deep hedging strategy with unweighted measure deviate from the analytical results further. Finally, portfolios with unweighted measure equal to one when the drift term is 0.6 and 1, i.e., large increment in the financial market. The results in Figure 5.10 to Figure 5.14 for negative drift terms draw similar curves but tend to a negative investment for low-price assets.

The occurrence of the weird shape on the left parts of the figures in Figure 5.4 to Figure 5.7 might be explained by Figure 5.8 and 5.9. Because the underlying asset prices are simulated by a Gaussian distribution, the network input samples that are priced in range 0 to 0.5 or to 0.75 lack. Thus, the FNN is not fully trained for low prices and produces these strange curves.

Note the figures for $\mu = 0.6$ have a better reweighted deep hedging result than the figures for $\mu = 0.3$ in Figure 5.3, 5.5 and 5.6. These two attempts with different drift terms are generated using the same value of λ . During training, the hedging strategy under a higher drift term deduces more empirical risks than the one with the lower μ . It may be caused by the huge utility function outcomes for large underlying asset prices with high drift. The hedging strategy reduces risk more efficient when the empirical loss is enlarged. When the neural network is fully trained, its output approaches the optimal solution. Also, the shifting turning points in the price range 0.5 to 0.75 for deep hedging strategies matches the moving input prices, Figure 5.5 and 5.6, caused by the positive drift term.

We are not taking $\lambda = 15$, which theoretically enables to achieve the best result, for all attempts. It is mainly because large risk aversion will lead to an explosive empirical risk loss. It is hard for computers to handle this huge loss and to train it down.

More figures with different μ and λ can be seen in Appendix A.1.

5.2 Deep Hedging and Measure Reweighting in Heston Model

Because the solution of martingale measure \mathbb{Q} for the Heston model is not unique, the result by Radon-Nikodym measure cannot be a numerical reference in this section. The given parameter and FNN settings for Black-Scholes remain unchanged. Some additional fixed parameters typically for the Heston model are introduced:

- Revert rate $\kappa = 0.3$
- Long-term volatility $\theta = 0.2$
- Correlation between Brownian motions $\rho = -0.2$
- Initial instantaneous volatility $V_0 = 0.2$

The risk aversion λ keeps as 10 for efficiency. The indifference price p in utility hedging exists as it was in the Black-Scholes model because it only affects the scale of loss during neural network training.

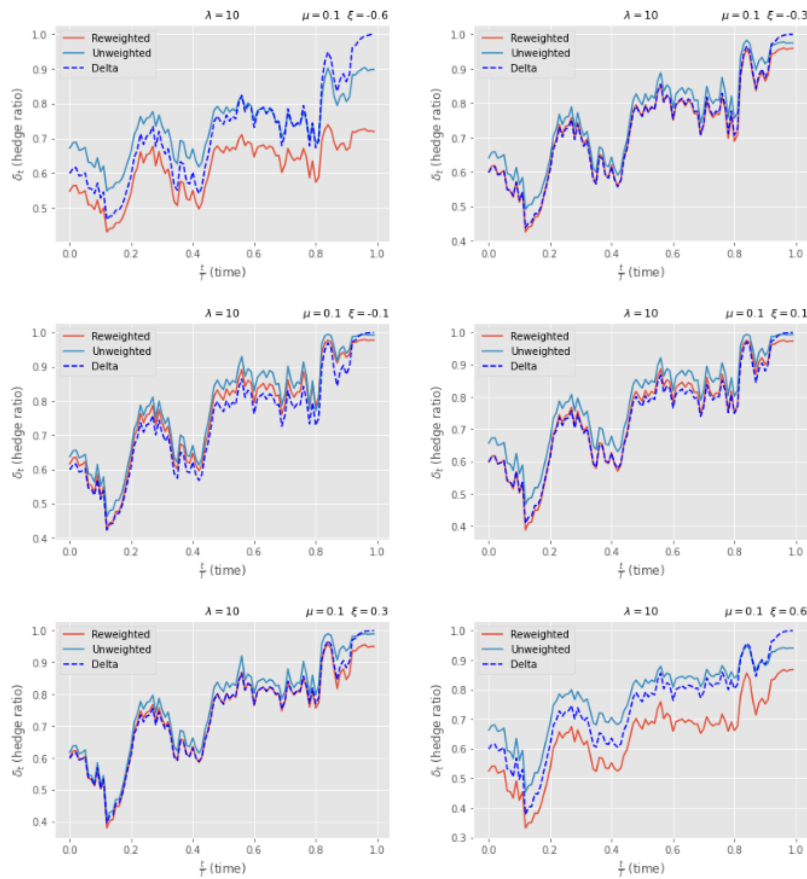


Figure 5.15: Heston model - Hedge European call option with $\mu = 0.1$ and $\lambda = 10$ for different volatility of instantaneous volatility ξ . The graphs are shown with respect to changes in time.

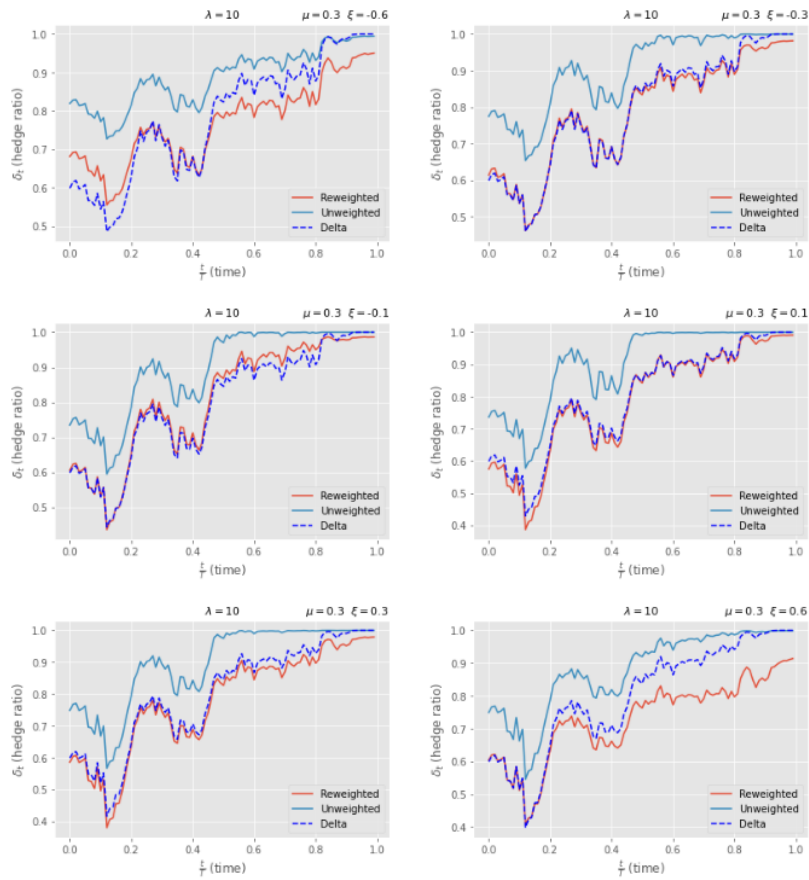


Figure 5.16: Heston model - Hedge European call option with $\mu = 0.3$ and $\lambda = 10$ for different volatility of instantaneous volatility ξ . The graphs are shown with respect to changes in time.

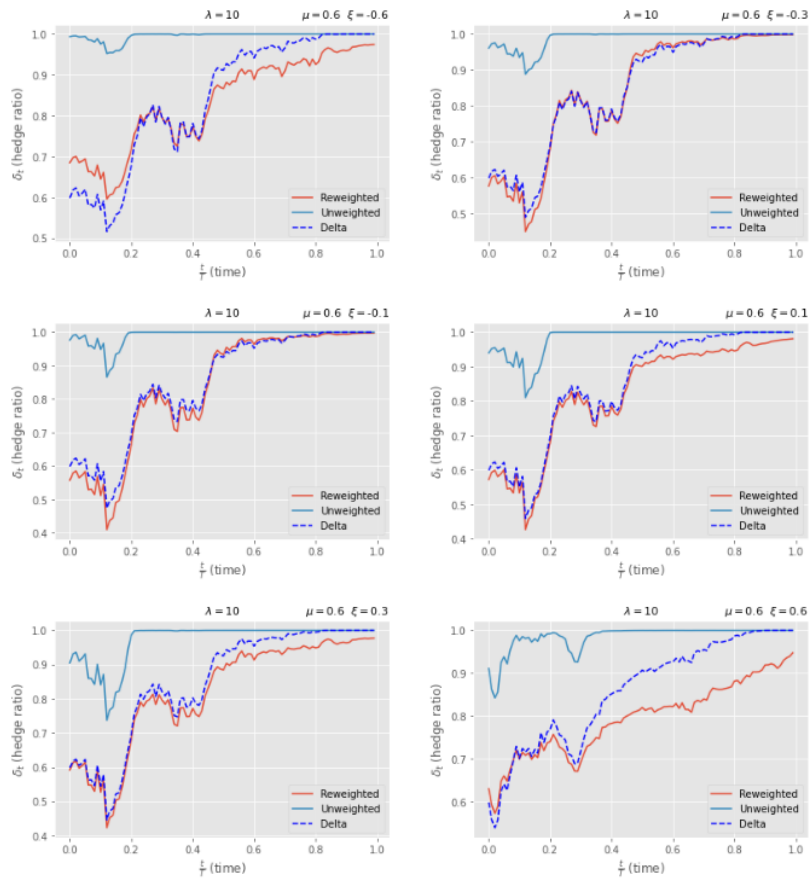


Figure 5.17: Heston model - Hedge European call option with $\mu = 0.6$ and $\lambda = 10$ for different volatility of instantaneous volatility ξ . The graphs are shown with respect to changes in time.

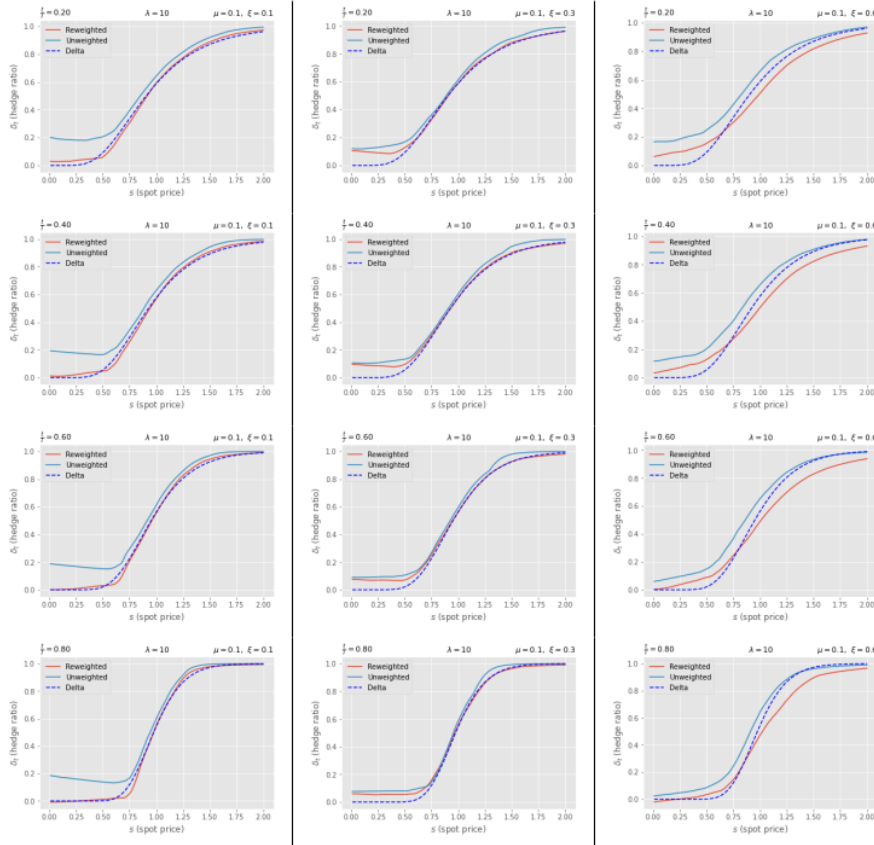


Figure 5.18: Heston model - Hedge European call option with $\mu = 0.1$, $\lambda = 10$ and different positive volatility of instantaneous volatility ξ .

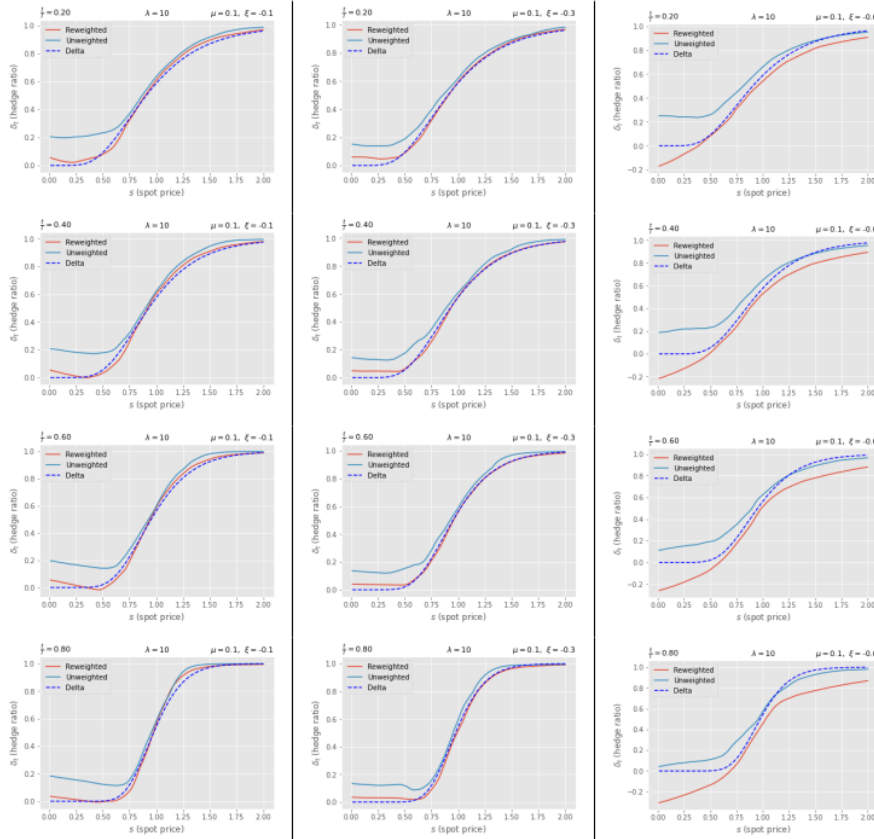


Figure 5.19: Heston model - Hedge European call option with $\mu = 0.1$, $\lambda = 10$ and different negative volatility of instantaneous volatility ξ .

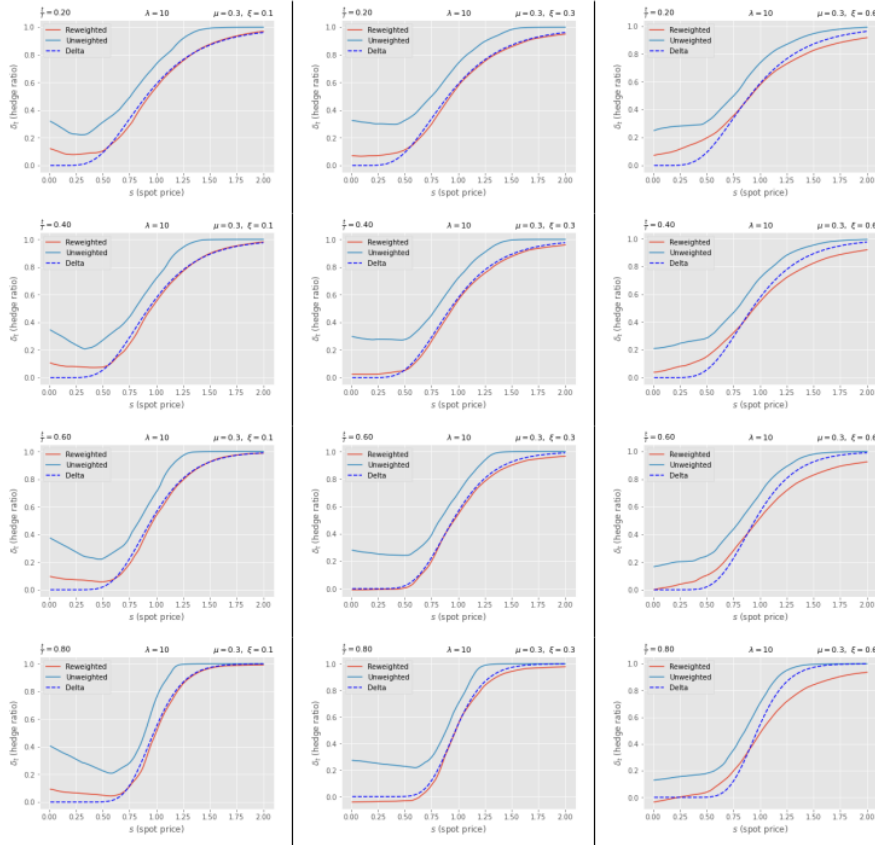


Figure 5.20: Heston model - Hedge European call option with $\mu = 0.3$, $\lambda = 10$ and different positive volatility of instantaneous volatility ξ .

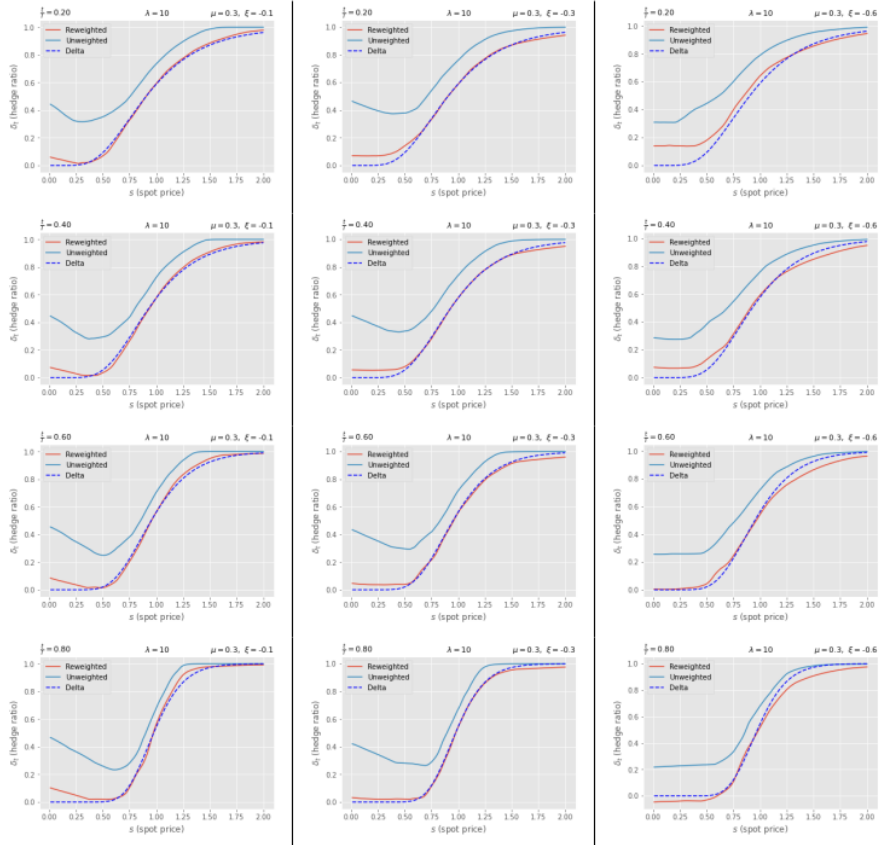


Figure 5.21: Heston model - Hedge European call option with $\mu = 0.3$, $\lambda = 10$ and different negative volatility of instantaneous volatility ξ .

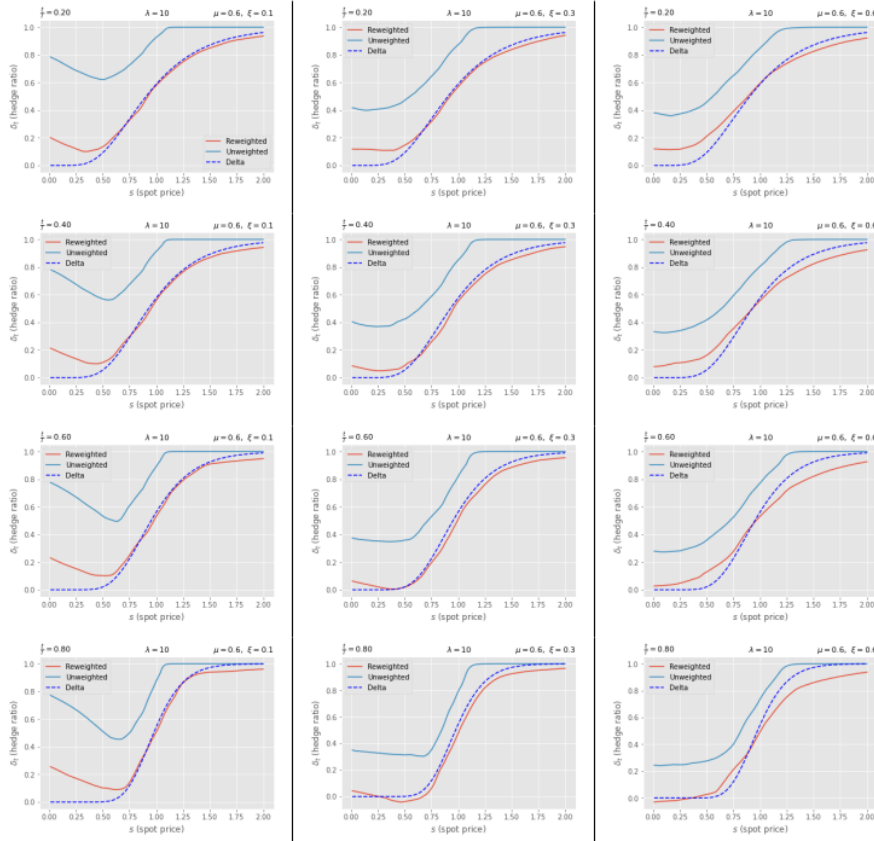


Figure 5.22: Heston model - Hedge European call option with $\mu = 0.6$, $\lambda = 10$ and different positive volatility of instantaneous volatility ξ .

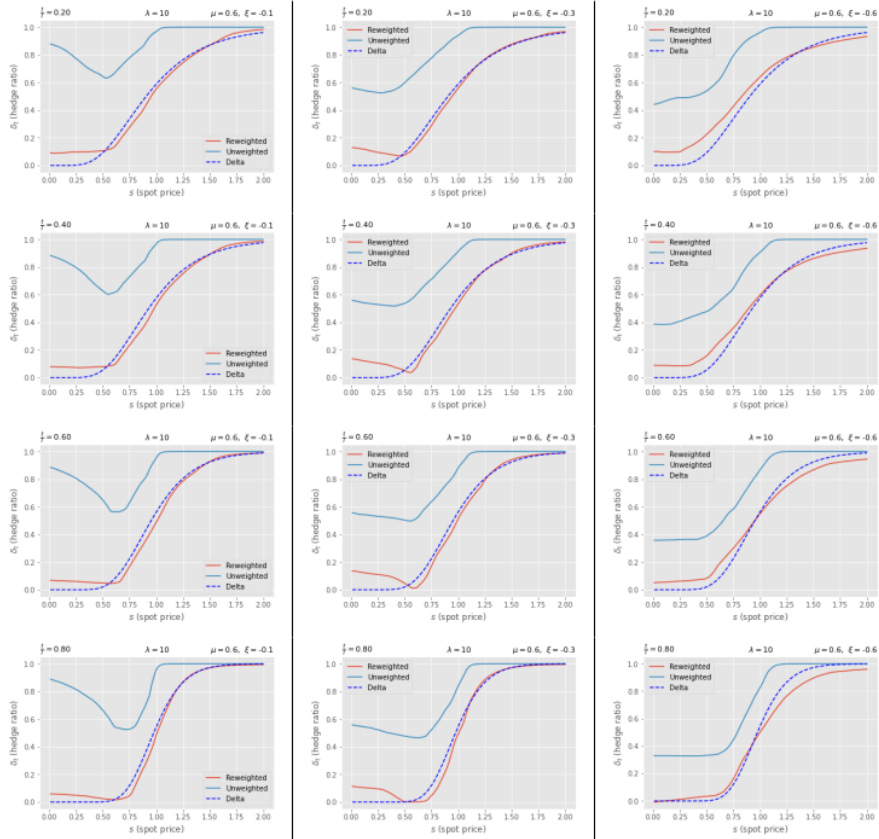


Figure 5.23: Heston model - Hedge European call option with $\mu = 0.6$, $\lambda = 10$ and different negative volatility of instantaneous volatility ξ .

The Heston model turns into a Black-Scholes model if $\theta = V_0$ and $\xi = 0$. The equation (4.1.1)

$$\begin{aligned} V_1^H &= V_0^H + \kappa(\theta - V_0^H)dt + \xi\sqrt{V_0^H}\zeta_0^V\sqrt{dt} \\ &= V_0 + \kappa(V_0 - V_0)dt + 0 \cdot \sqrt{V_0^H}\zeta_0^V\sqrt{dt} \\ &= V_0 \end{aligned}$$

Thus, by induction, one can have

$$V_t^H = V_0$$

and the underlying asset price

$$\begin{aligned} S_{t+1}^H &= S_t^H \exp\left(\left(\mu - \frac{V_0}{2}\right)dt + \sqrt{V_0}\zeta_t^S\sqrt{dt}\right) \\ &= S_t^H \exp\left((\mu - c)dt + c' \cdot \zeta_t^S\sqrt{dt}\right) \end{aligned}$$

Where c and c' represent constants. This case is tested as for validation purpose but does not present the result in this paper (which hold the same results as in Section 5.1).

From Figure 5.15 to 5.23, it shows that the result of deep hedge options becomes flat when the volatility of instantaneous volatility increases. The changes in curves indicate that: the investors are required to spend most of their cash on the high valued underlying assets when ξ is around zero; the hedging portfolio lifts the weight for low valued underlying assets when the absolute value of ξ becomes large.

The figures, especially in Figure 5.17, 5.22 and 5.23, show that the deep hedging strategy with unweighted measure approaching to one during neural network training as it does with the Black-Scholes model. As a comparison, strategy with reweighted asset path probability results a reasonable and reliable output.

Remark 5.2.1. The blue dash-line curves in figures are calculated by Black-Scholes delta hedging. It is placed just for reference instead of an analytical solution.

More figures with different μ , ξ and λ can be seen in Appendix A.2.

5.3 Black-Scholes Model with Realized Volatility

Buehler et al. [8] have written in their paper that the deep hedging strategy can be applied to a Black-Scholes market, where underlying assets and at the money Puts and Calls can be traded at each time step, for illustrating the effect of the measure change. Hence, besides simulating the underlying prices, a related European call option is generated as well. The option is priced with a volatility value different from the one for underlying asset price simulation. In this case, there is an effective statistical arbitrage between the underlying asset and the option. For transforming

the market to an adapted version for deep hedging, one may reweight the underlying asset paths' measure.

The basic settings are similar as the one in Section 5.1, but the market is free of drift with variable volatility:

- Stochastic volatility for underlying assets $\sigma^{realized}$
- Stochastic volatility for European call options $\sigma^{implied}$

and the FNN structure

$$f \in \mathcal{N}_4(3, 100, 100, 100, 1; \text{ReLU}, \text{ReLU}, \text{ReLU}, \text{linear})$$

The FNN has inputs: time, underlying asset price and call option price. The *linear* in the output layer represents the activation function converts into an affine function.

Remark 5.3.1. Be careful to use *linear* as the output layer activation function. This function is unbounded. Thus, it may cause a jump in losses when training the neural network and results a failure.

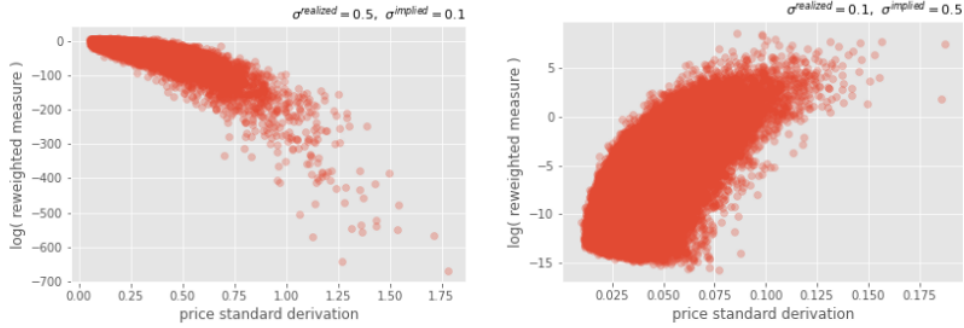


Figure 5.24: Black-Scholes model - Scatter Plot of the standard deviation for underlying asset price (i.e., the realized volatility $\sigma^{realized}$) and the trained reweighted measure

The figure on the left in Figure 5.24 represents the case $\sigma^{implied} < \sigma^{realized}$. It demonstrates that paths with low realized volatility are low weighted and paths with high realized volatility are high weighted. A counter result is shown from the figure on the right with situation $\sigma^{implied} > \sigma^{realized}$ that the asset path weight increases when the realized volatility increases.

Because high implied volatility generates highly stochastic option paths, the reweighted measure is influenced more by the prices of the option. So the right-hand-side figure in Figure 5.24 has a more dispersed shape than the left one.

5.4 Pairs Trading on Real Funds

In the real financial market, sometimes one can apply pairs trading strategy on two funds. These two funds are typically doing simultaneous movements, i.e., either increase or decrease their price in the same percentages at the same time, for a long period of time. The instability between two funds may increase due to the chasing ups and downs done by investors or the miss-pricing caused by market makers, but a stable mean value exists for the spread between two funds to oscillate around. These two funds can be said as mathematically cointegrated. Pairs trading is the strategy that utilizes the spread price divergence. For example, when the instantaneous spread is positive and higher than its mean value, investors sell the fund with higher price; when the instantaneous spread is positive but lower than its mean value, investors buy the fund with lower price. Unlike many other trading strategies, pairs trading is a risk-neutral trading strategy.

We may consider that the measure reweighting is similar to the pairs strategy. Both of them do cancellation on the effective statistical arbitrage between two financial derivatives. As we use deep learning to train for a new measure of two derivatives, the structure of FNN may keep the same as in Section 5.3

$$f \in \mathcal{N}_4(3, 100, 100, 100, 1; \text{ReLU}, \text{ReLU}, \text{ReLU}, \text{linear})$$

If there is a purpose for bounded outcomes, the activation function in the output layer can use *Hyperbolic tangent*.

A one-year data in seconds of two funds is used here: the Vanguard 500 Index Fund (VOO) and the iShares Core S&P 500 Index Fund (IVV) [15]. The raw data I used is a pre-processed data (pre-processed by my supervisor Dr Mikko Pakkanen) which is collected from the first to the last trading date in year 2020 and separated by two minutes. The final dataset gained is a set of prices with 48259 asset paths and 120 time steps (i.e., 120 seconds) for each fund.

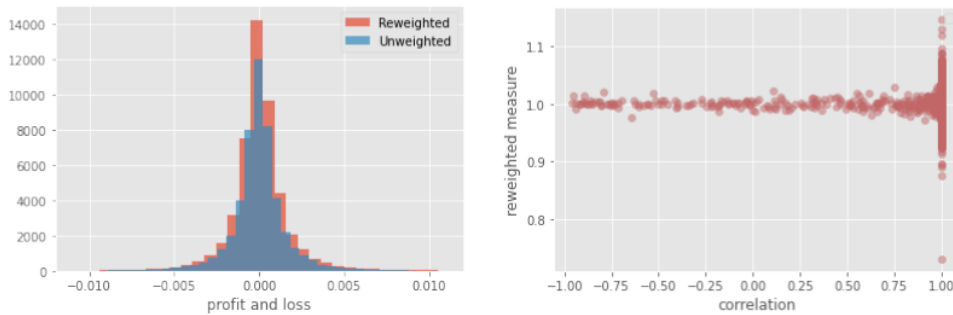


Figure 5.25: The histogram of profit and loss with reweighted measure and the scatter plot of two funds correlation and their reweighted measure.

The shape of profit and loss, histogram in Figure 5.25, although the statistical arbitrage in funds VOO and IVV are small, the deep hedging strategy with reweighted

measure results more concentrate, which agrees free of statistical arbitrage. Different from the results assumed in Section 5.3, scatter plots in Figure 5.25 and 5.26 reveal that there is no relationship between the trained reweighted measure and the highly correlated (most values of correlation between VOO and IVV are equal to one) and cointegrated (most p-values for cointegration between VOO and IVV are nearly zero) price paths.

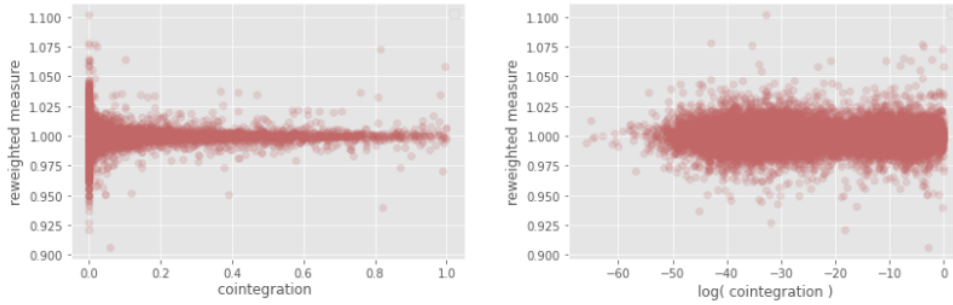


Figure 5.26: The scatter plots of two funds correlation (p-value based on MacKinnon [17]) and their different-scaled reweighted measure.

With an attempt of finding how the trained measure works (Table 5.1), it is found that the result does not follow the pairs strategy. The portfolio generated under the measure-reweighting-like strategy is long together and short together.

VOO	7.8535438	2.7456868	-1.577576	-2.4031937	-4.8154325	-5.388236
IVV	13.704949	5.2937264	-1.206552	-2.4244452	-5.0658345	-5.685785

Table 5.1: Few fragments of the trained reweighted measure for the path gains the highest profit and loss.

Combined with Figure 5.27, price paths for VOO and IVV have almost the same shape of lines with a value around 3×10^6 but with tiny changes in units of 10^2 (Figure 5.28 is the spreads when investing the same amount of cash into both funds). The spreads are too small comparing with their price value. A more significant spread price between VOO and IVV, which is suitable for pairs trading, might be found with datasets in smaller time steps (e.g., millisecond-to-millisecond).

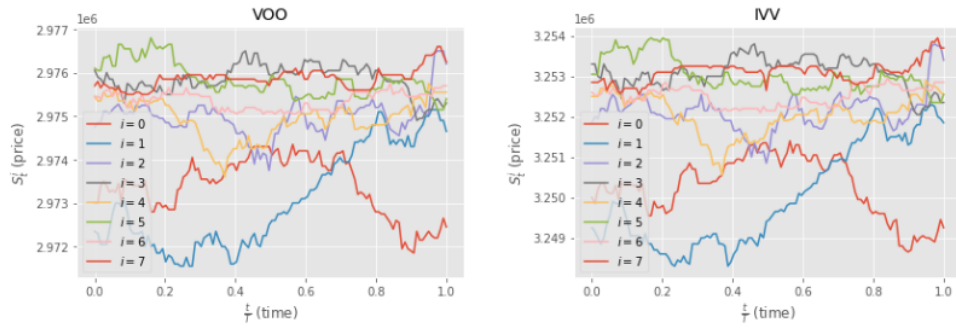


Figure 5.27: Related price paths of fund VOO and IVV with maturity $T = 2\text{min}$. Data was collected seconds-by-seconds in year 2020

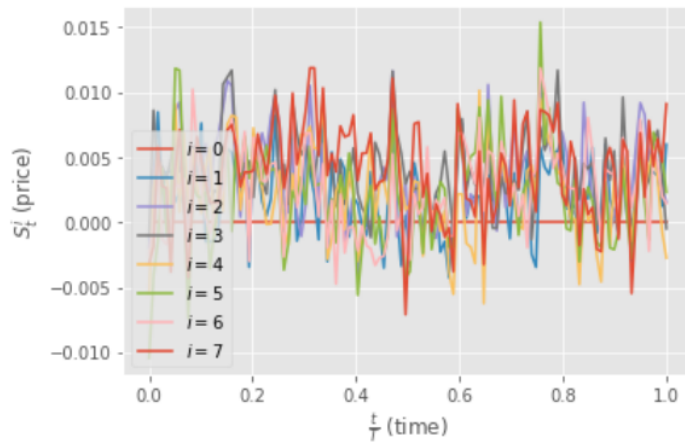


Figure 5.28: Price path differences between fund VOO and IVV with maturity $T = 2\text{min}$ by investing same number of shares. Data was collected seconds-by-seconds in year 2020

Chapter 6

Conclusion

In the Black-Scholes model, the traditional deep hedging strategy (i.e., equally-weighted on each asset price based on Buehler et al. [7]) performs well when the market prices are adapted or slowly increased/decreased in its overall trend (i.e., the absolute value of drift term μ is small). However, the trading strategy is equally buying underlying assets when the market has a trend with a sharp gradient, which is unrealistic in reality. For applying the deep hedging strategy to reality, this paper introduces one type of solution by changing the measure of the market. The new market measure enables underlying prices to be measurable and can be generated by either analytical Radon-Nikodym density calculation or by measure reweighting method.

It testifies that both the Radon-Nikodym measure and reweighted measure improve the traditional deep hedging strategy and make it reliable under most of the cases in the Black-Scholes model. Even if there is no accessible analytical reference (e.g., in the Heston model), the deep hedging strategy with reweighted measure results reasonable and reliable.

For showing the influence of measure reweighting, a test of hedging between underlying assets and their related options. The volatility of the options, called the implied volatility, is not aligned with the one of underlying assets. It is found that the scale of the reweighted measure has a monotonic relationship to the realized volatility, i.e., the volatility of the underlying asset. When $\sigma^{implied} > \sigma^{realized}$, the trend between the reweighted measure and realized volatility is monotonically increasing; and when $\sigma^{implied} < \sigma^{realized}$, the trend between the reweighted measure and realized volatility is monotonically decreasing.

Pairs trading is a practical case that operating similarly to measure reweighting as they are both making market risk-neutral. However, although the paths for fund VOO and IVV are highly correlated and cointegrated, the result we got does not like what pairs strategy should present. The failure might be caused by the tiny scale of the spread between two funds in our dataset.

Further attempts could be made to simulate more underlying prices with a wider time range or to find the most reasonable value of λ for each drift term in the Black-Scholes model. For further study of the pairs trading case, it is suggested to try

either new funds with more significant spreads or a VOO and IVV price dataset with smaller time steps (e.g., millisecond-to-millisecond).

Appendix A

Additional Figures

A.1 Figures for Black-Scholes model

A.1.1 Figures with $\lambda = 1$

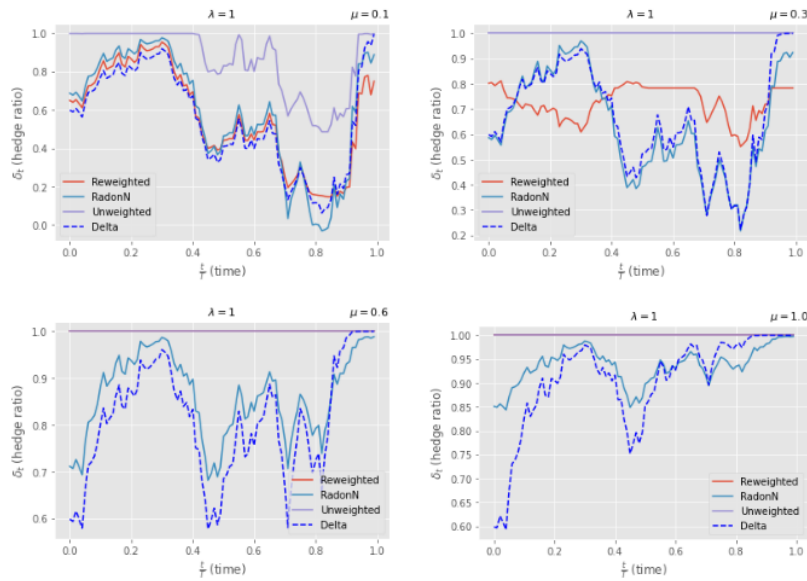


Figure A.1: Black-Scholes model - Hedge European call option with $\lambda = 1$ for different positive μ . The graphs are shown with respect to changes in time.

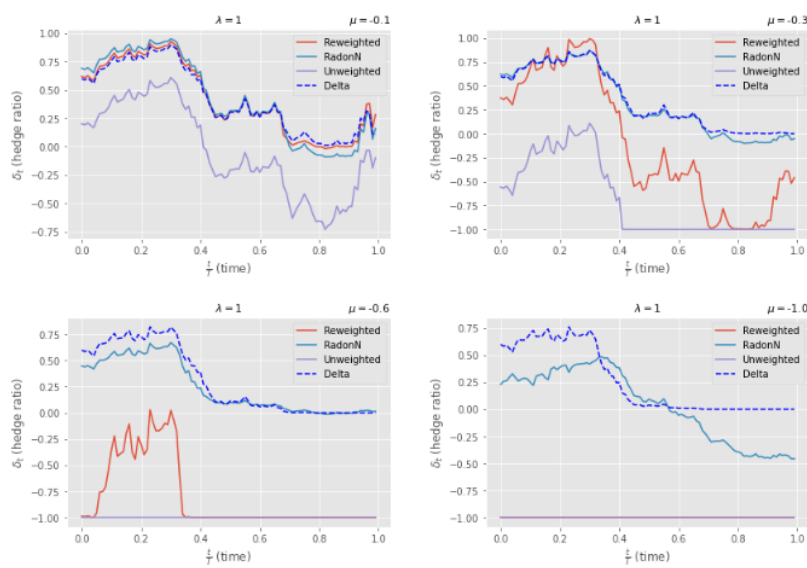


Figure A.2: Black-Scholes model - Hedge European call option with $\lambda = 1$ for different negative μ . The graphs are shown with respect to changes in time.

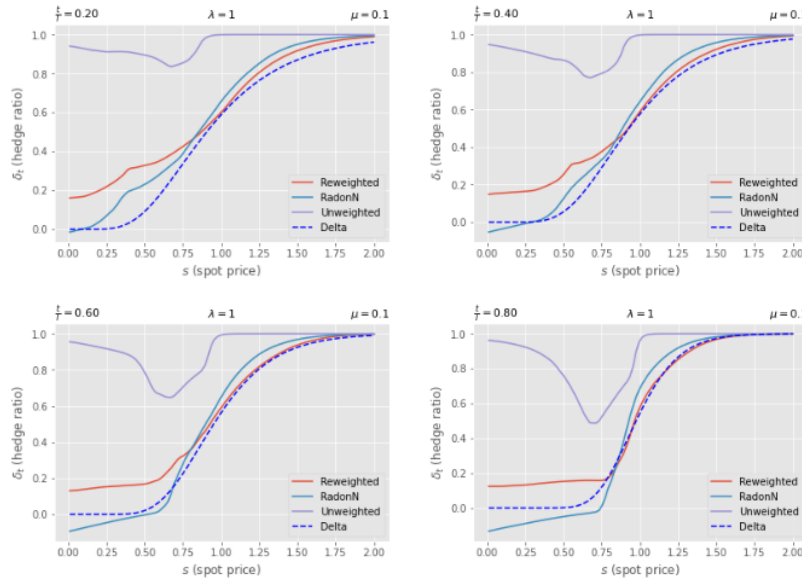


Figure A.3: Black-Scholes model - Comparison of the hedge ratio between deep hedging strategy with reweighted, Radon-Nikodym and unweighted measure and the delta hedging strategy with $\lambda = 1$ and $\mu = 0.1$

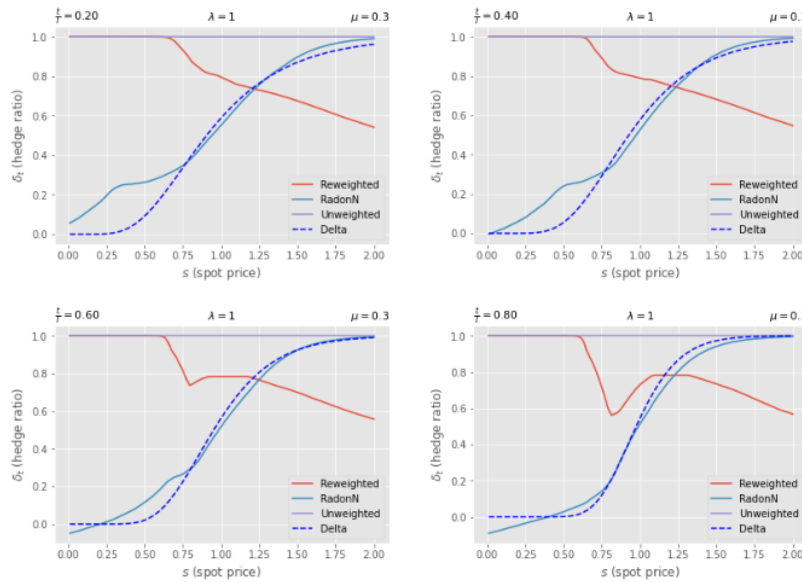


Figure A.4: Black-Scholes model - Comparison of the hedge ratio between deep hedging strategy with reweighted, Radon-Nikodym and unweighted measure and the delta hedging strategy with $\lambda = 1$ and $\mu = 0.3$

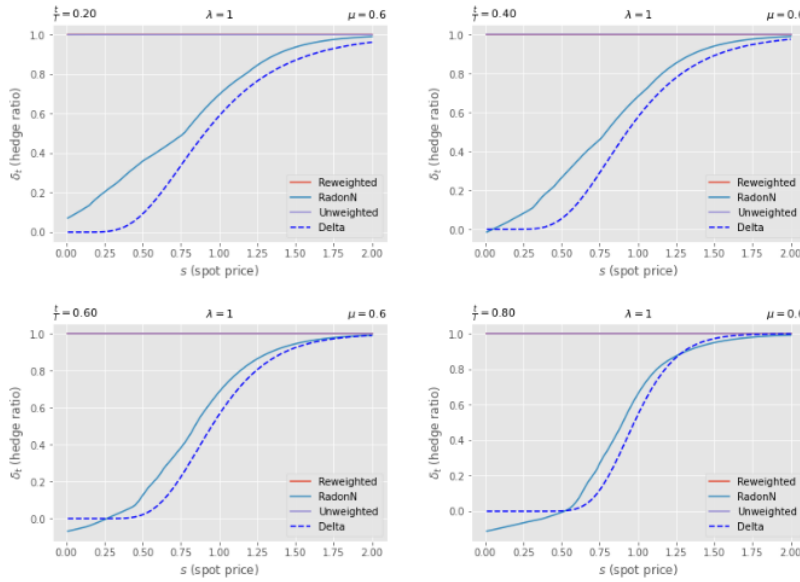


Figure A.5: Black-Scholes model - Comparison of the hedge ratio between deep hedging strategy with reweighted, Radon-Nikodym and unweighted measure and the delta hedging strategy with $\lambda = 1$ and $\mu = 0.6$

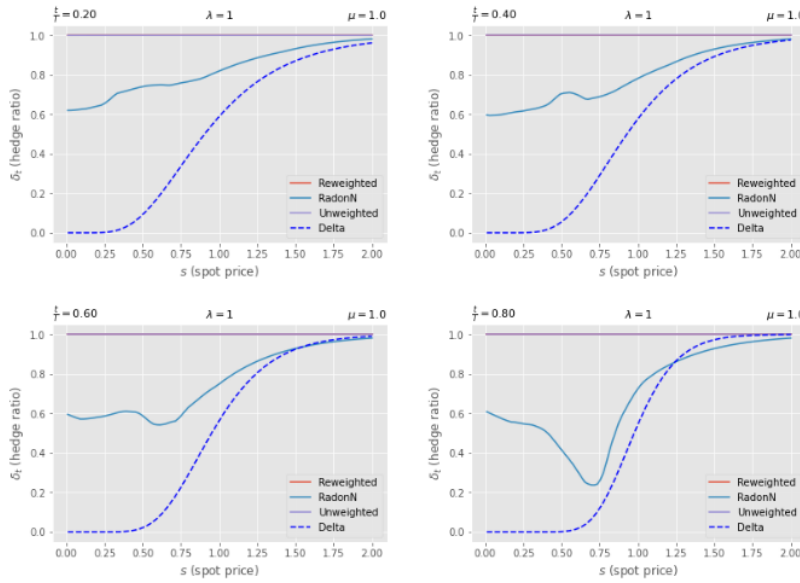


Figure A.6: Black-Scholes model - Comparison of the hedge ratio between deep hedging strategy with reweighted, Radon-Nikodym and unweighted measure and the delta hedging strategy with $\lambda = 1$ and $\mu = 1.0$

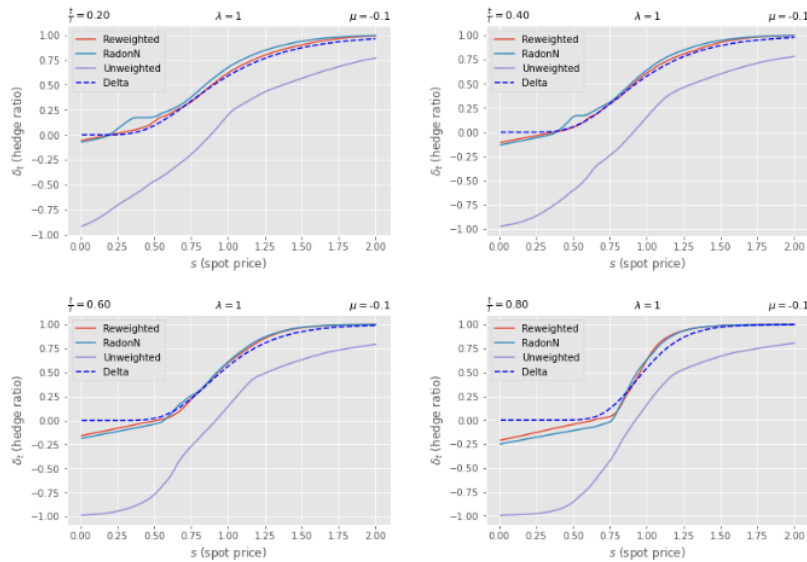


Figure A.7: Black-Scholes model - Comparison of the hedge ratio between deep hedging strategy with reweighted, Radon-Nikodym and unweighted measure and the delta hedging strategy with $\lambda = 1$ and $\mu = -0.1$

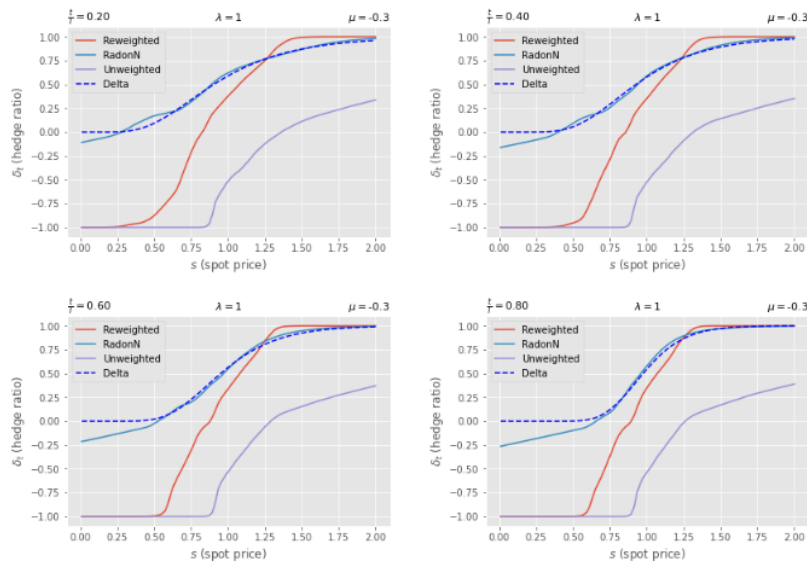


Figure A.8: Black-Scholes model - Comparison of the hedge ratio between deep hedging strategy with reweighted, Radon-Nikodym and unweighted measure and the delta hedging strategy with $\lambda = 1$ and $\mu = -0.3$

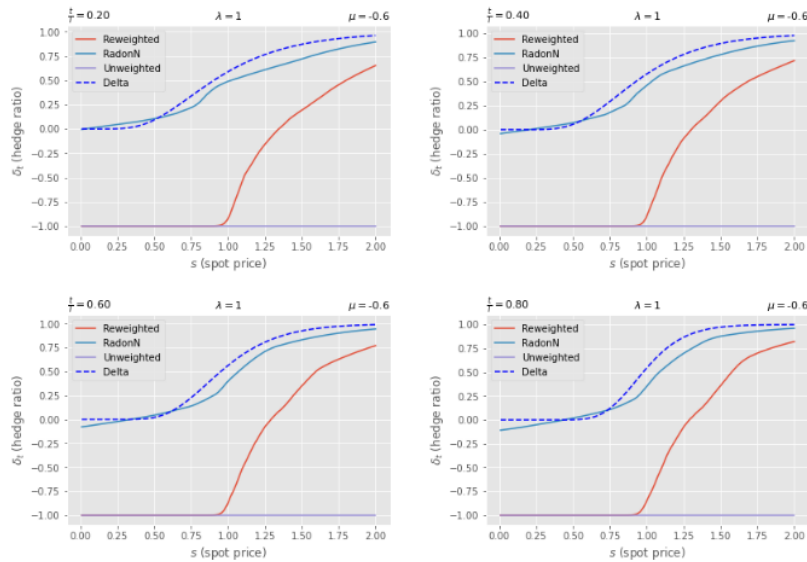


Figure A.9: Black-Scholes model - Comparison of the hedge ratio between deep hedging strategy with reweighted, Radon-Nikodym and unweighted measure and the delta hedging strategy with $\lambda = 1$ and $\mu = -0.6$

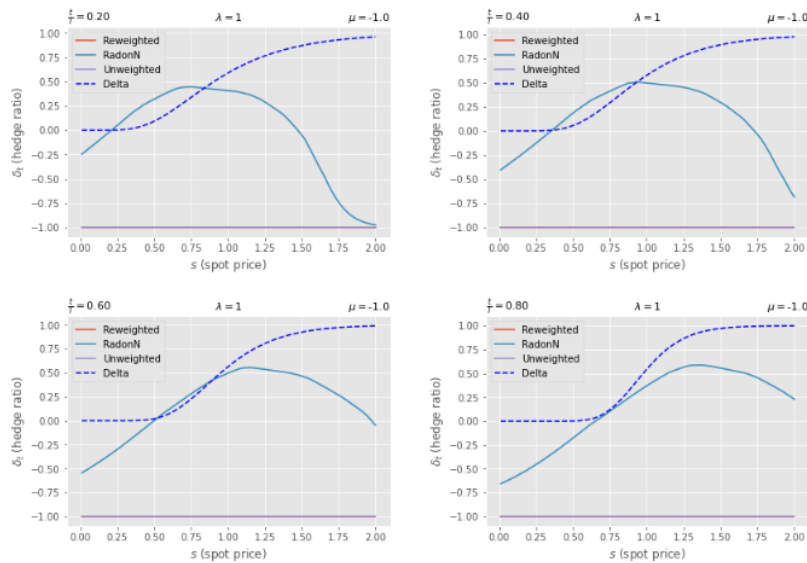


Figure A.10: Black-Scholes model - Comparison of the hedge ratio between deep hedging strategy with reweighted, Radon-Nikodym and unweighted measure and the delta hedging strategy with $\lambda = 1$ and $\mu = -1.0$

A.1.2 Figures with $\lambda = 5$

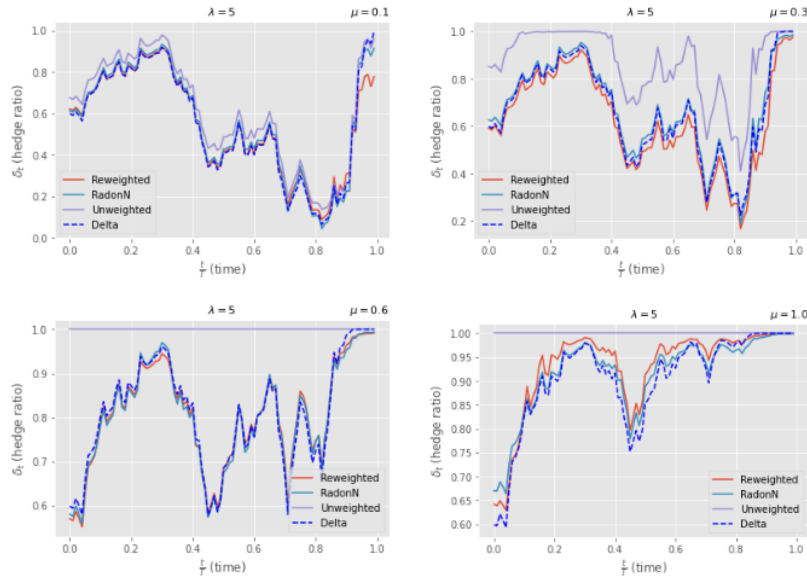


Figure A.11: Black-Scholes model - Hedge European call option with $\lambda = 5$ for different positive μ . The graphs are shown with respect to changes in time.

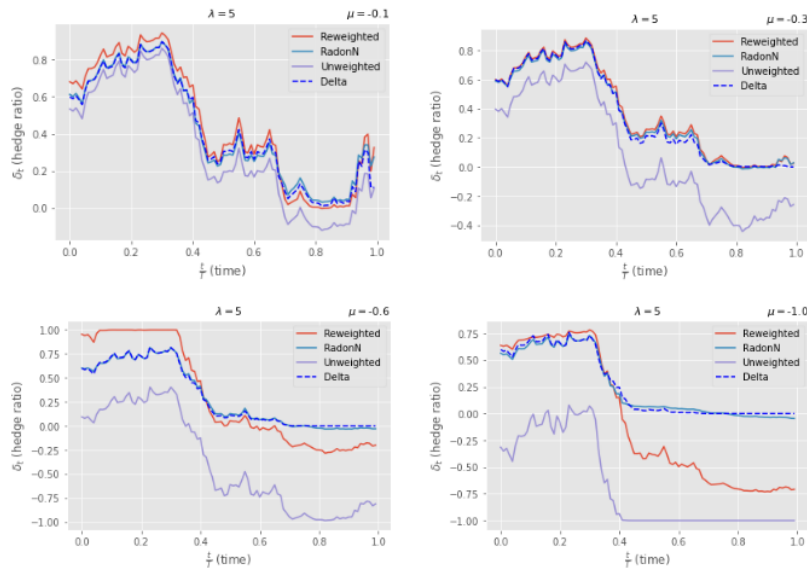


Figure A.12: Black-Scholes model - Hedge European call option with $\lambda = 5$ for different negative μ . The graphs are shown with respect to changes in time.

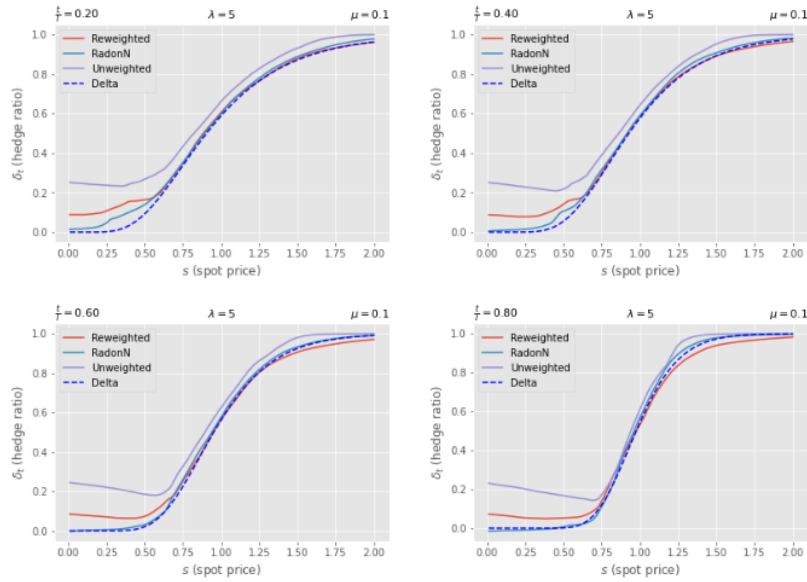


Figure A.13: Black-Scholes model - Comparison of the hedge ratio between deep hedging strategy with reweighted, Radon-Nikodym and unweighted measure and the delta hedging strategy with $\lambda = 5$ and $\mu = 0.1$

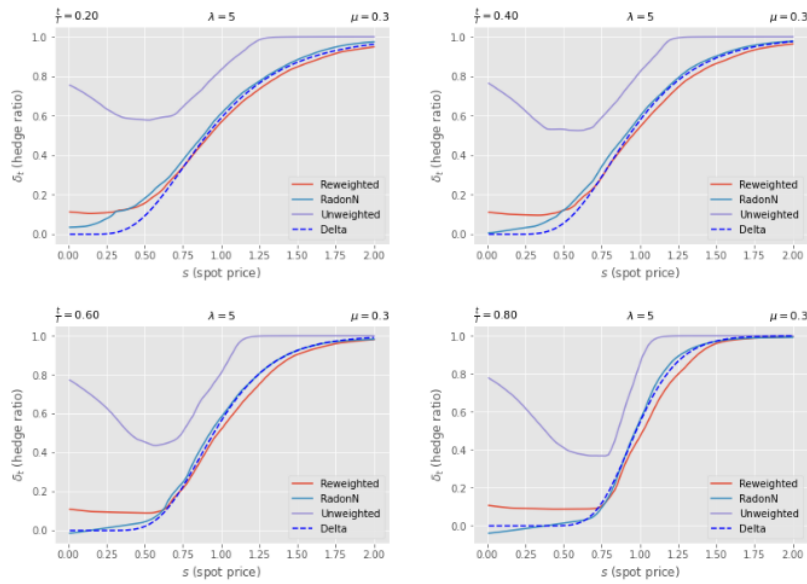


Figure A.14: Black-Scholes model - Comparison of the hedge ratio between deep hedging strategy with reweighted, Radon-Nikodym and unweighted measure and the delta hedging strategy with $\lambda = 5$ and $\mu = 0.3$

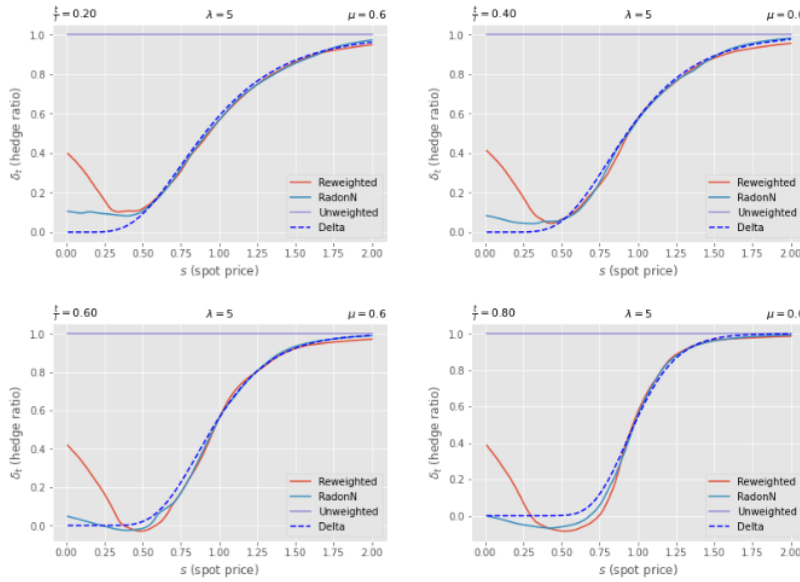


Figure A.15: Black-Scholes model - Comparison of the hedge ratio between deep hedging strategy with reweighted, Radon-Nikodym and unweighted measure and the delta hedging strategy with $\lambda = 5$ and $\mu = 0.6$

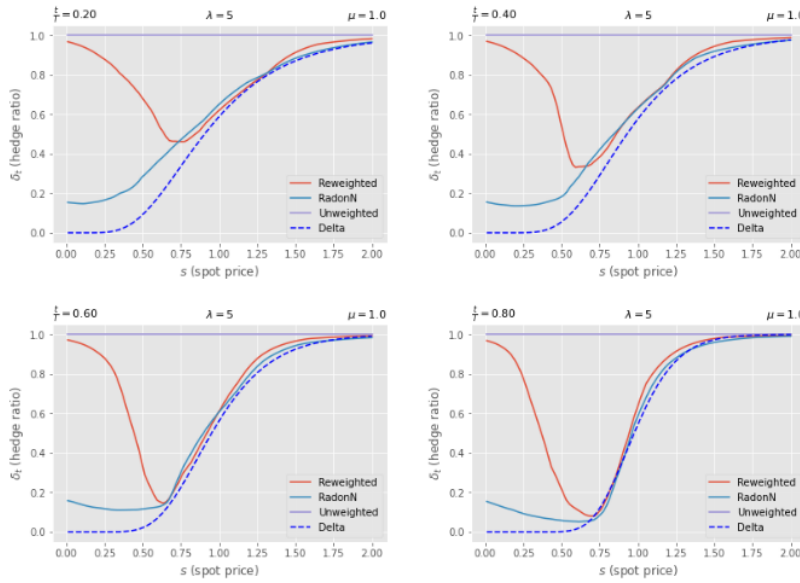


Figure A.16: Black-Scholes model - Comparison of the hedge ratio between deep hedging strategy with reweighted, Radon-Nikodym and unweighted measure and the delta hedging strategy with $\lambda = 5$ and $\mu = 1.0$

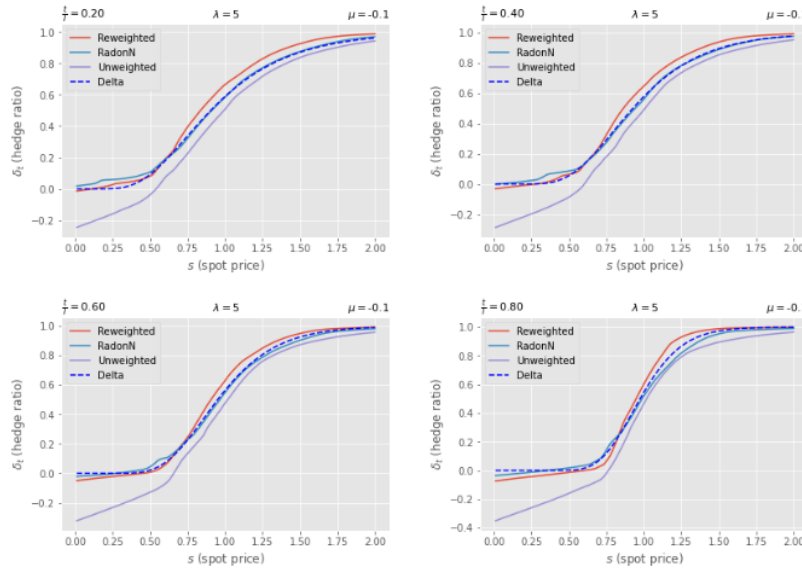


Figure A.17: Black-Scholes model - Comparison of the hedge ratio between deep hedging strategy with reweighted, Radon-Nikodym and unweighted measure and the delta hedging strategy with $\lambda = 5$ and $\mu = -0.1$

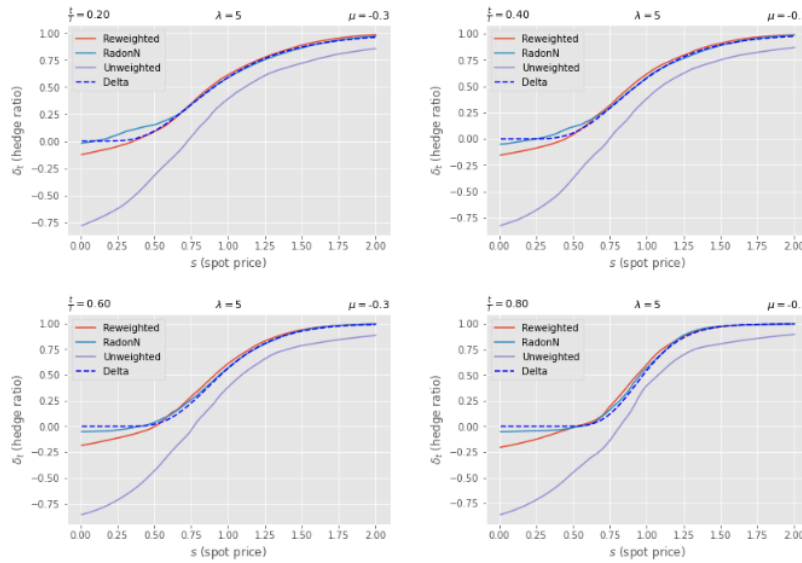


Figure A.18: Black-Scholes model - Comparison of the hedge ratio between deep hedging strategy with reweighted, Radon-Nikodym and unweighted measure and the delta hedging strategy with $\lambda = 5$ and $\mu = -0.3$

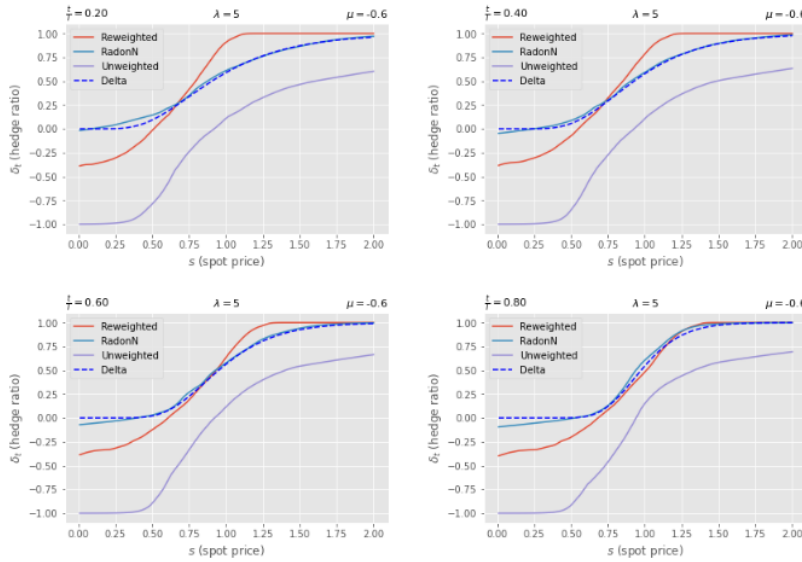


Figure A.19: Black-Scholes model - Comparison of the hedge ratio between deep hedging strategy with reweighted, Radon-Nikodym and unweighted measure and the delta hedging strategy with $\lambda = 5$ and $\mu = -0.6$

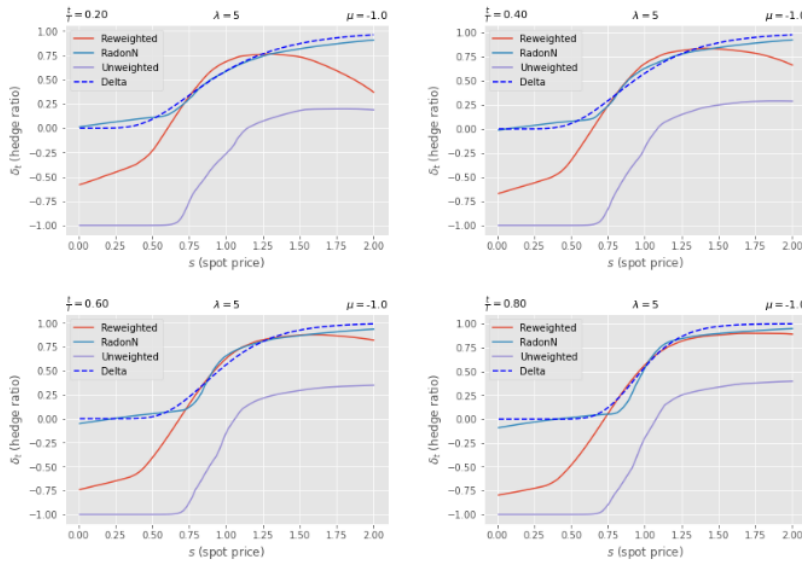


Figure A.20: Black-Scholes model - Comparison of the hedge ratio between deep hedging strategy with reweighted, Radon-Nikodym and unweighted measure and the delta hedging strategy with $\lambda = 5$ and $\mu = -1.0$

A.2 Figures for Heston model

A.2.1 Figures with $\lambda = 1$

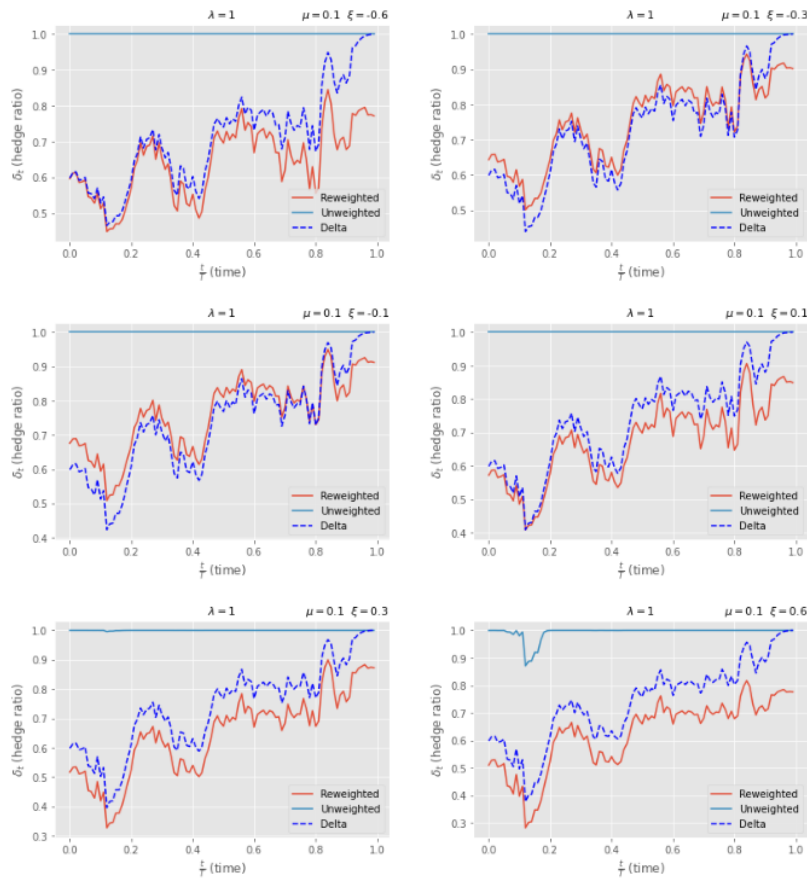


Figure A.21: Heston model - Hedge European call option with $\mu = 0.1$, $\lambda = 1$ and different volatility of instantaneous volatility ξ . The graphs are shown with respect to changes in time.

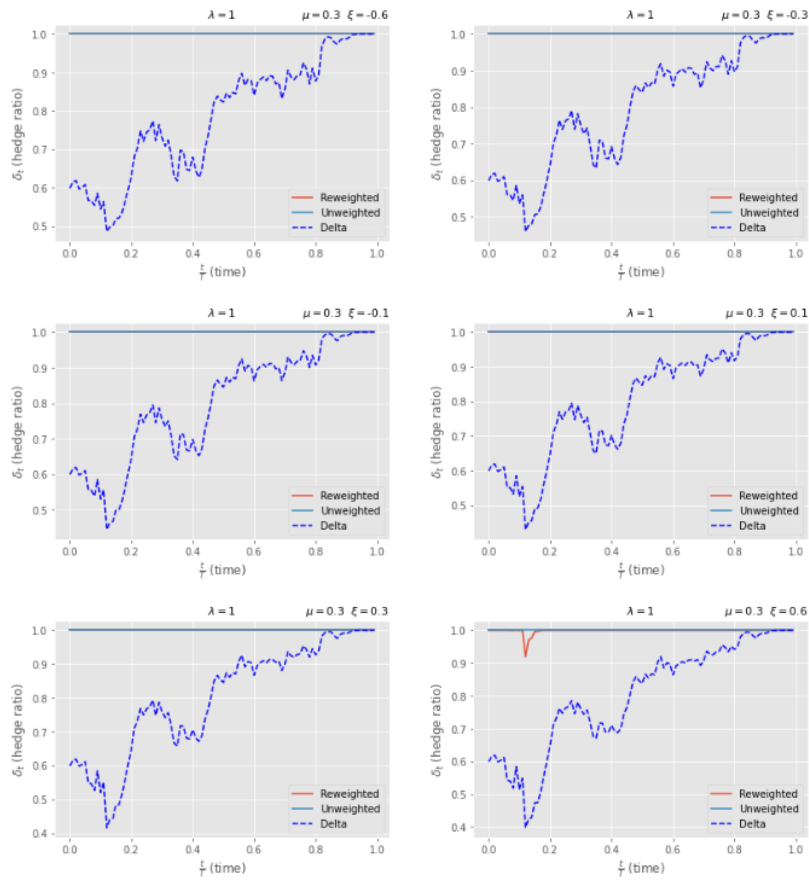


Figure A.22: Heston model - Hedge European call option with $\mu = 0.3$, $\lambda = 1$ and different volatility of instantaneous volatility ξ . The graphs are shown with respect to changes in time.

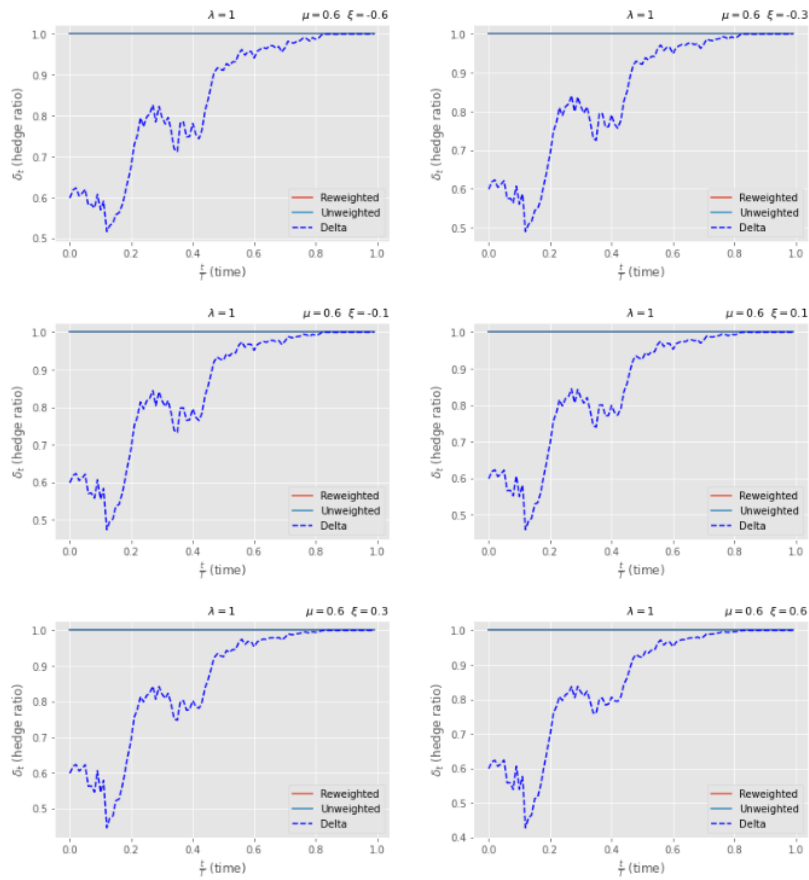


Figure A.23: Heston model - Hedge European call option with $\mu = 0.6$, $\lambda = 1$ and different volatility of instantaneous volatility ξ . The graphs are shown with respect to changes in time.

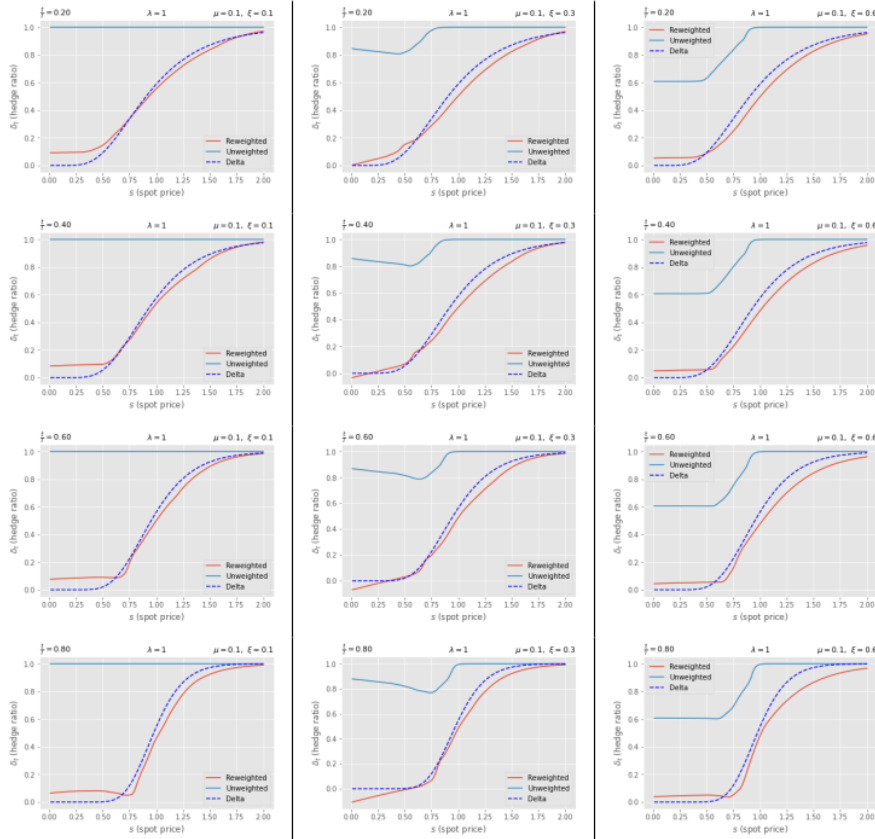


Figure A.24: Heston model - Hedge European call option with $\mu = 0.1$, $\lambda = 1$ and different positive volatility of instantaneous volatility ξ .

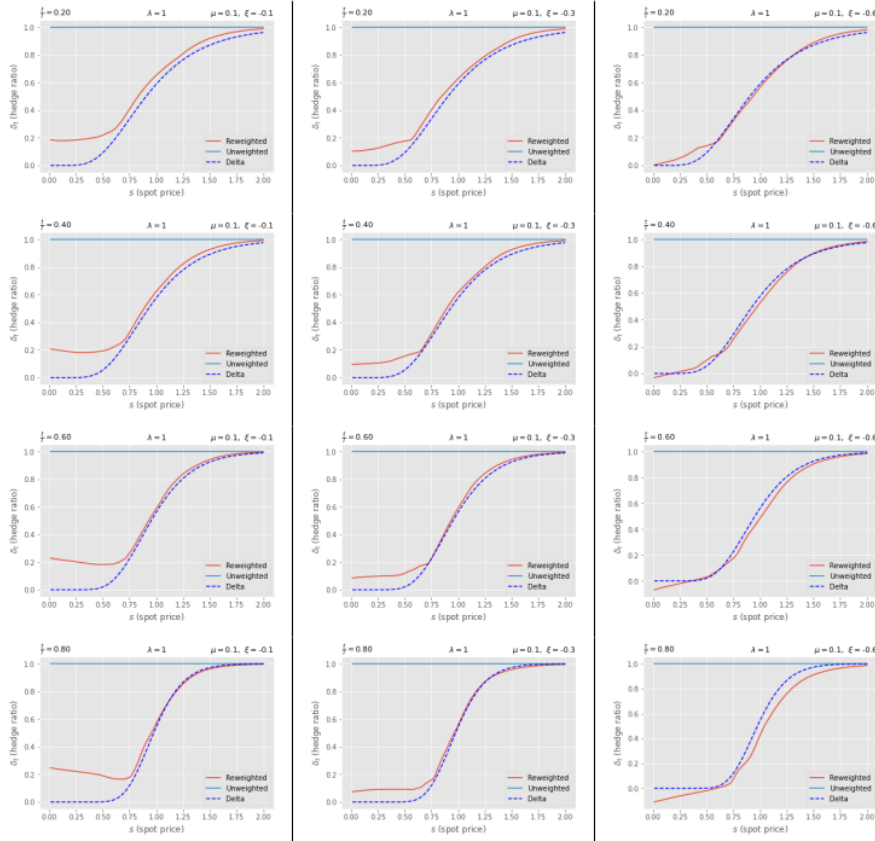


Figure A.25: Heston model - Hedge European call option with $\mu = 0.1$, $\lambda = 1$ and different negative volatility of instantaneous volatility ξ .

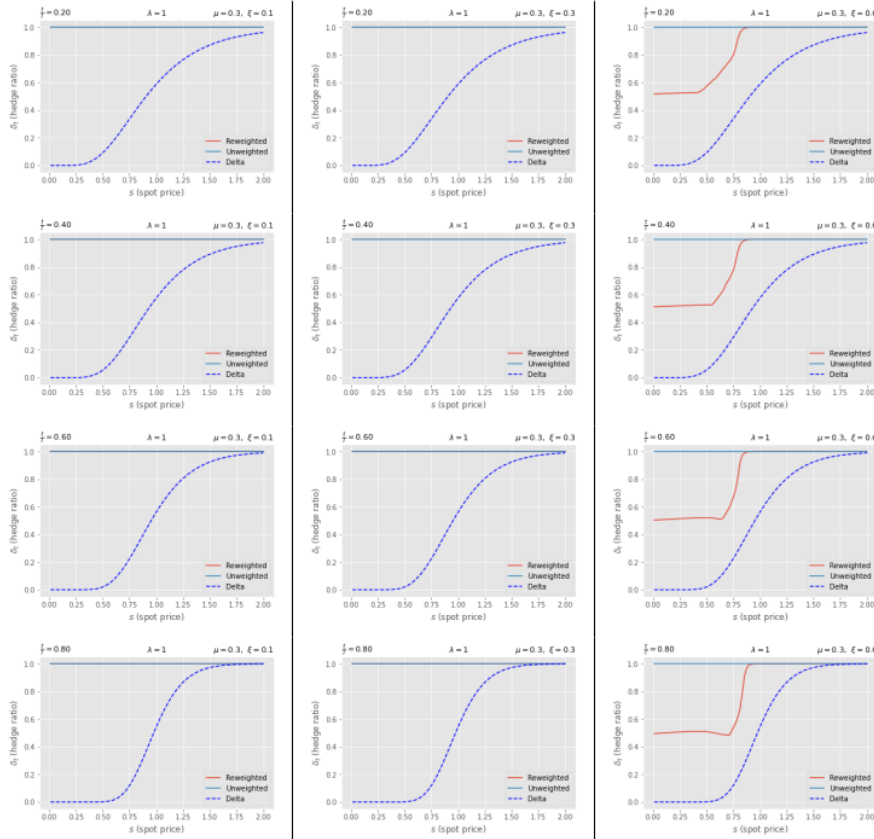


Figure A.26: Heston model - Hedge European call option with $\mu = 0.3$, $\lambda = 1$ and different positive volatility of instantaneous volatility ξ .

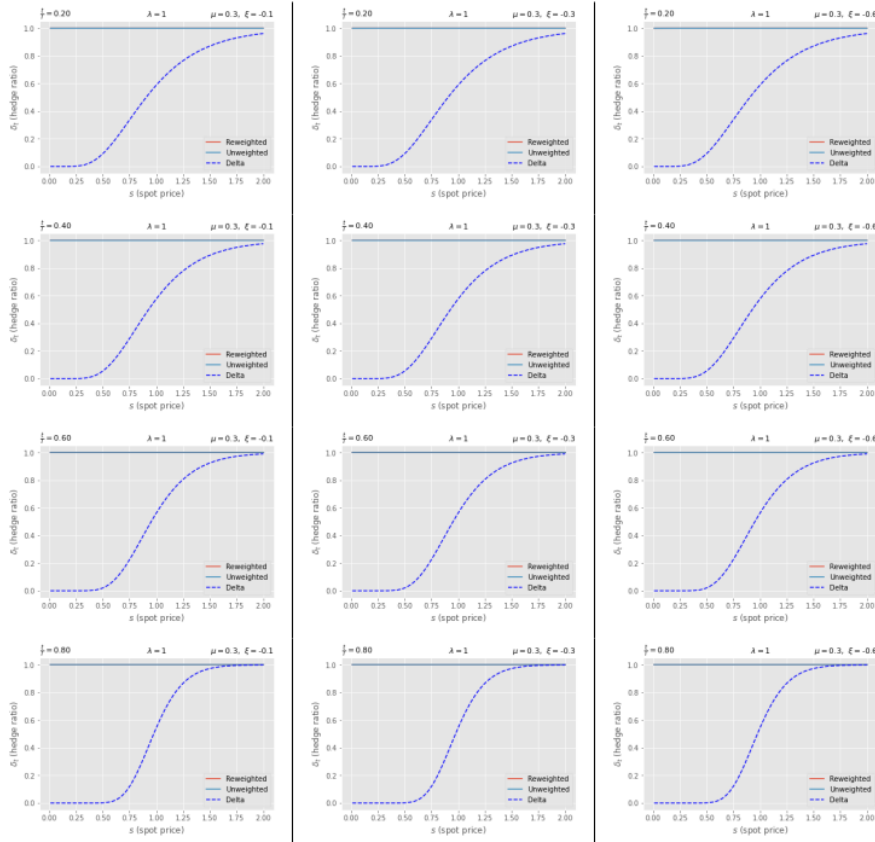


Figure A.27: Heston model - Hedge European call option with $\mu = 0.3$, $\lambda = 1$ and different negative volatility of instantaneous volatility ξ .

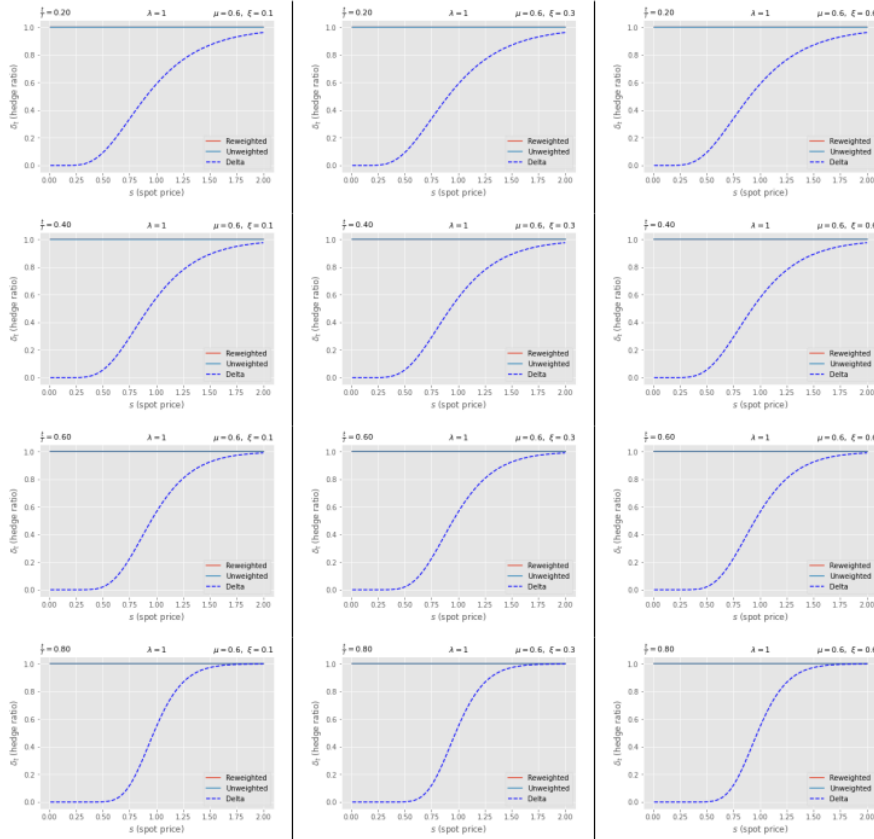


Figure A.28: Heston model - Hedge European call option with $\mu = 0.6$, $\lambda = 1$ and different positive volatility of instantaneous volatility ξ .

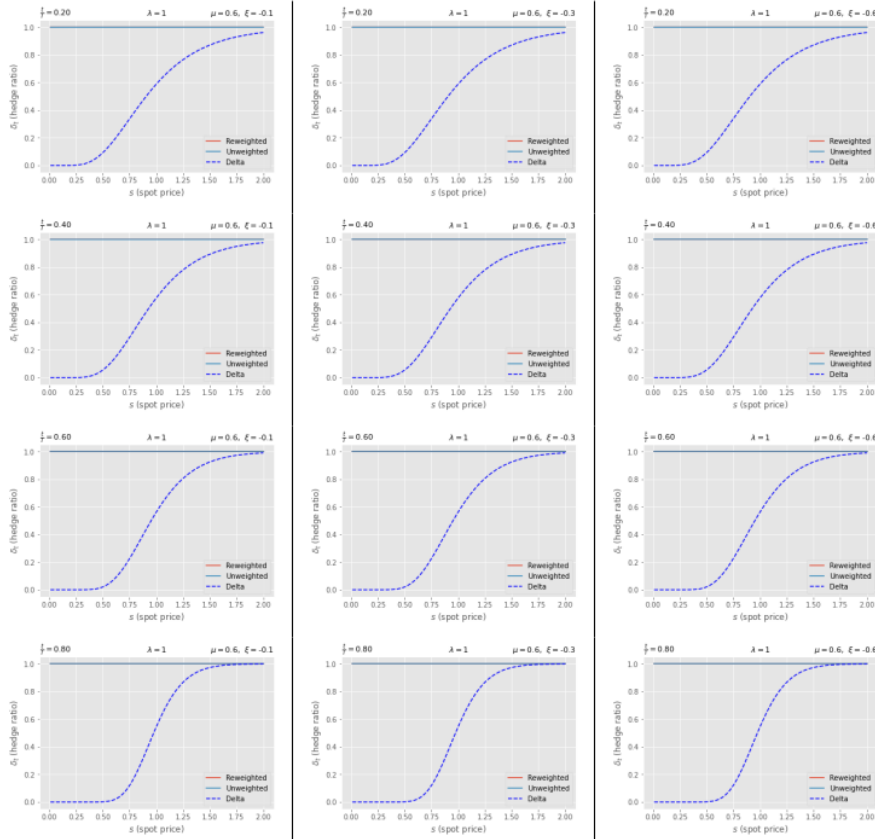


Figure A.29: Heston model - Hedge European call option with $\mu = 0.6$, $\lambda = 1$ and different negative volatility of instantaneous volatility ξ .

A.2.2 Figures with $\lambda = 5$

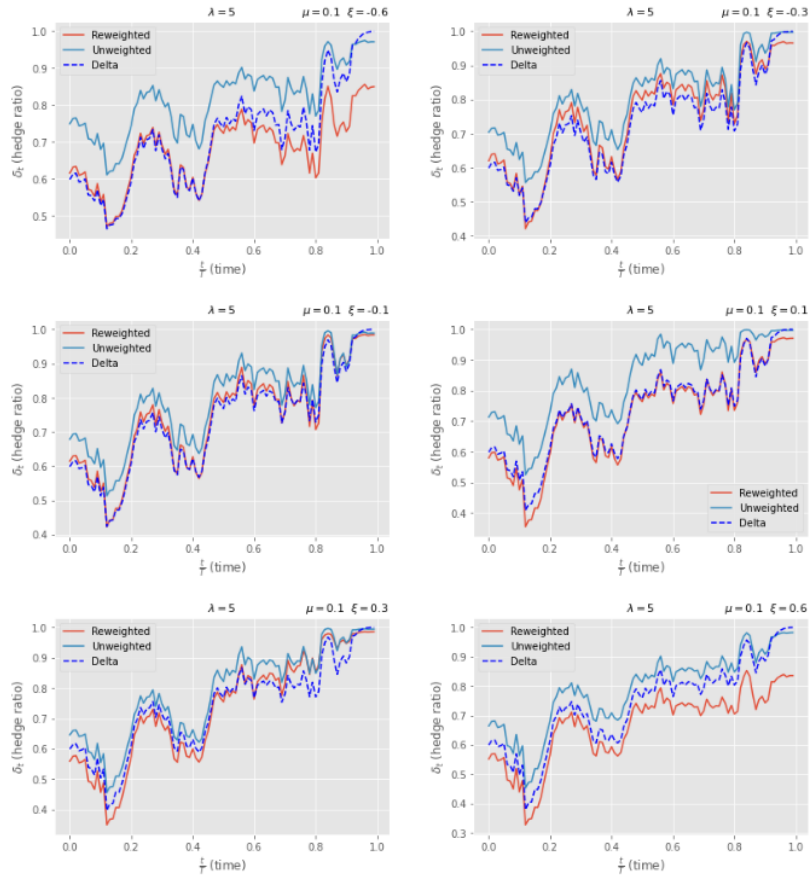


Figure A.30: Heston model - Hedge European call option with $\mu = 0.1$, $\lambda = 5$ and different volatility of instantaneous volatility ξ . The graphs are shown with respect to changes in time.

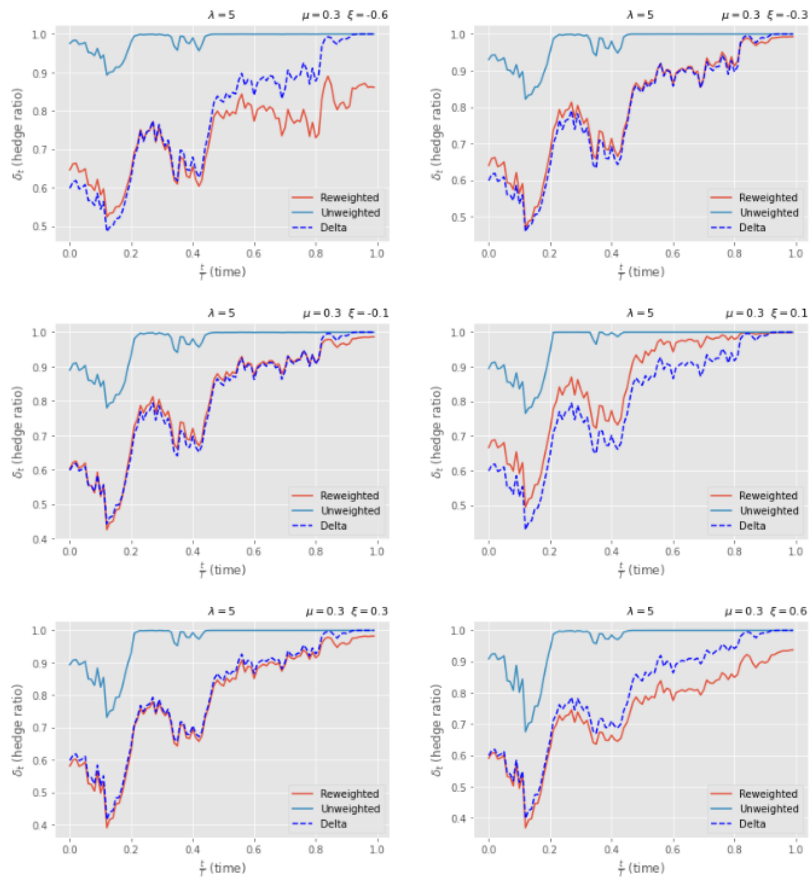


Figure A.31: Heston model - Hedge European call option with $\mu = 0.3$, $\lambda = 5$ and different volatility of instantaneous volatility ξ . The graphs are shown with respect to changes in time.

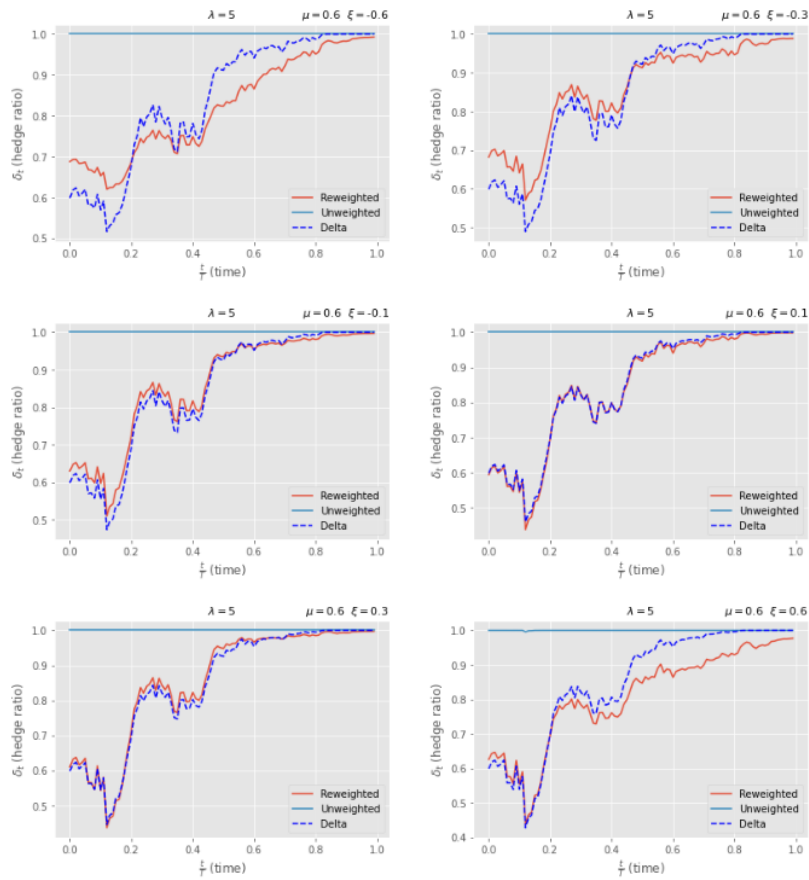


Figure A.32: Heston model - Hedge European call option with $\mu = 0.6$, $\lambda = 5$ and different volatility of instantaneous volatility ξ . The graphs are shown with respect to changes in time.

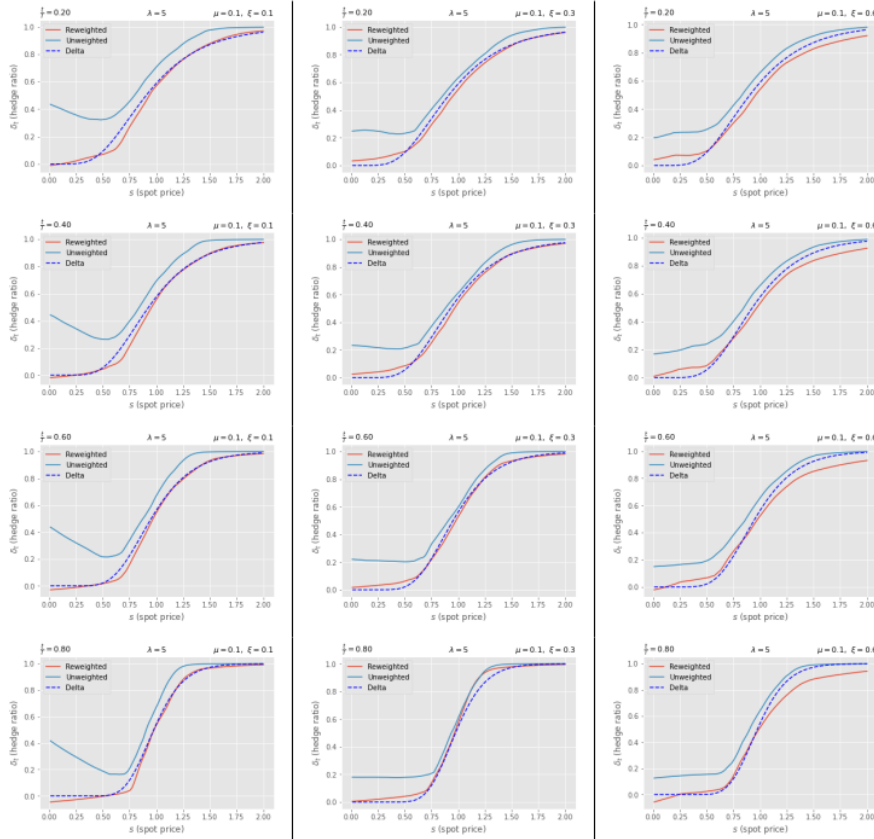


Figure A.33: Heston model - Hedge European call option with $\mu = 0.1$, $\lambda = 5$ and different positive volatility of instantaneous volatility ξ .

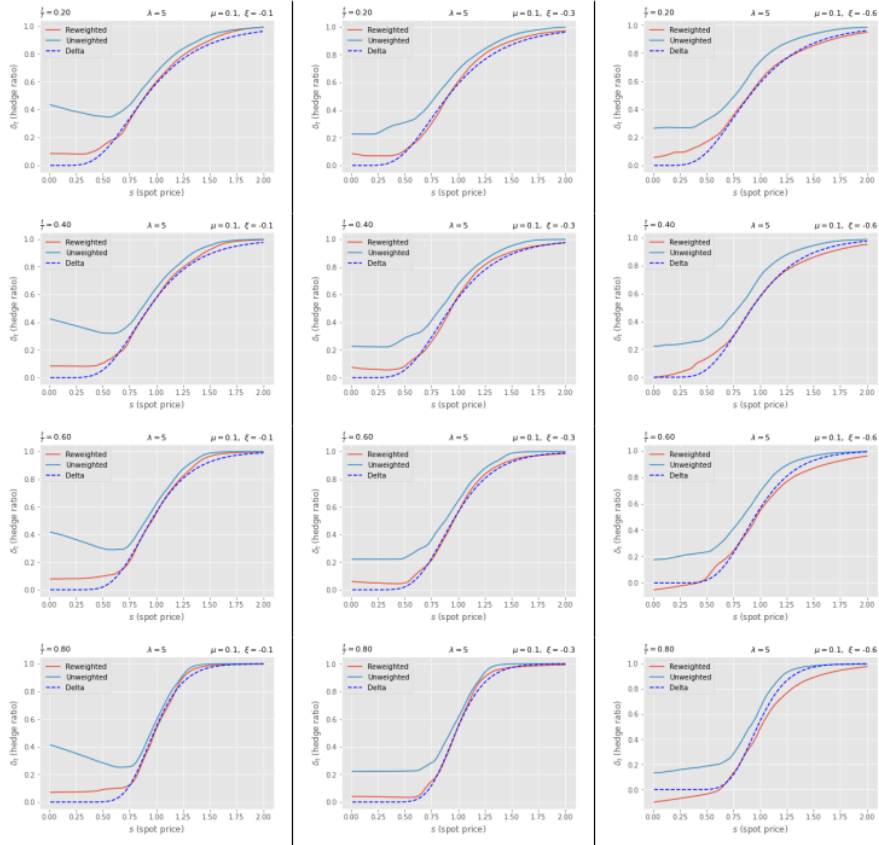


Figure A.34: Heston model - Hedge European call option with $\mu = 0.1$, $\lambda = 5$ and different negative volatility of instantaneous volatility ξ .

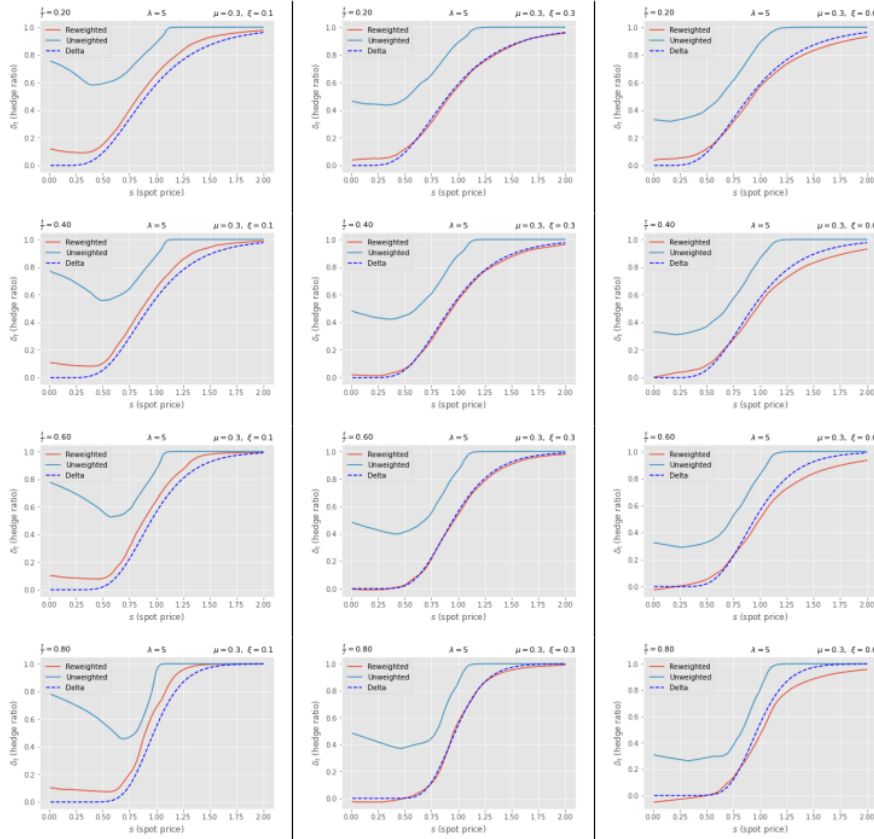


Figure A.35: Heston model - Hedge European call option with $\mu = 0.3$, $\lambda = 5$ and different positive volatility of instantaneous volatility ξ .

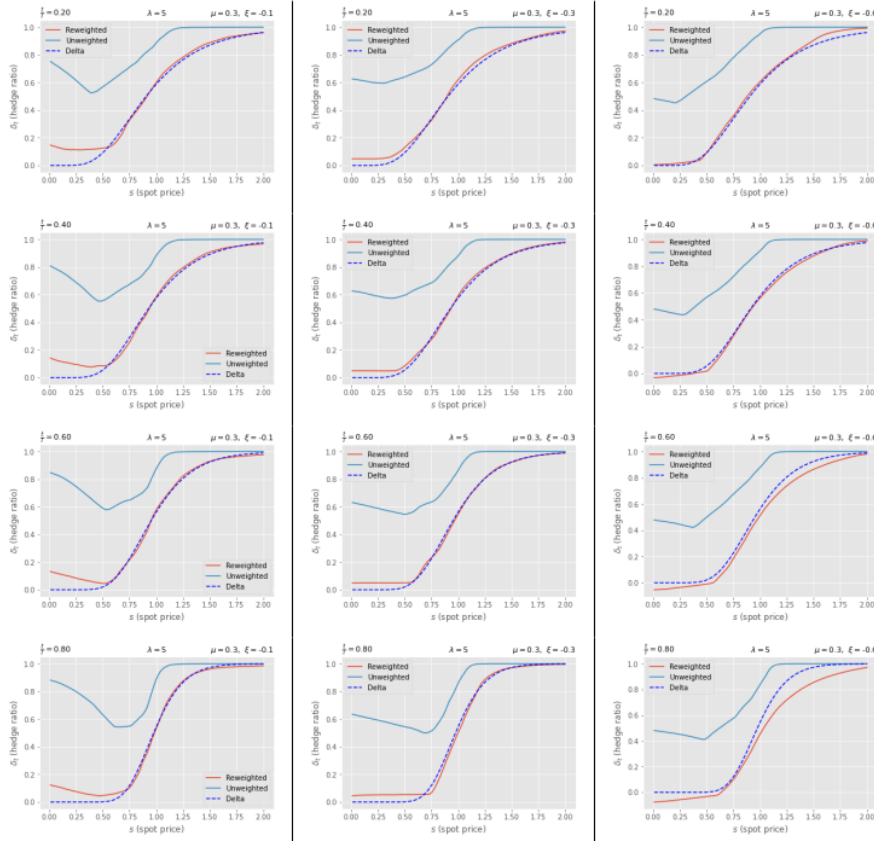


Figure A.36: Heston model - Hedge European call option with $\mu = 0.3$, $\lambda = 5$ and different negative volatility of instantaneous volatility ξ .

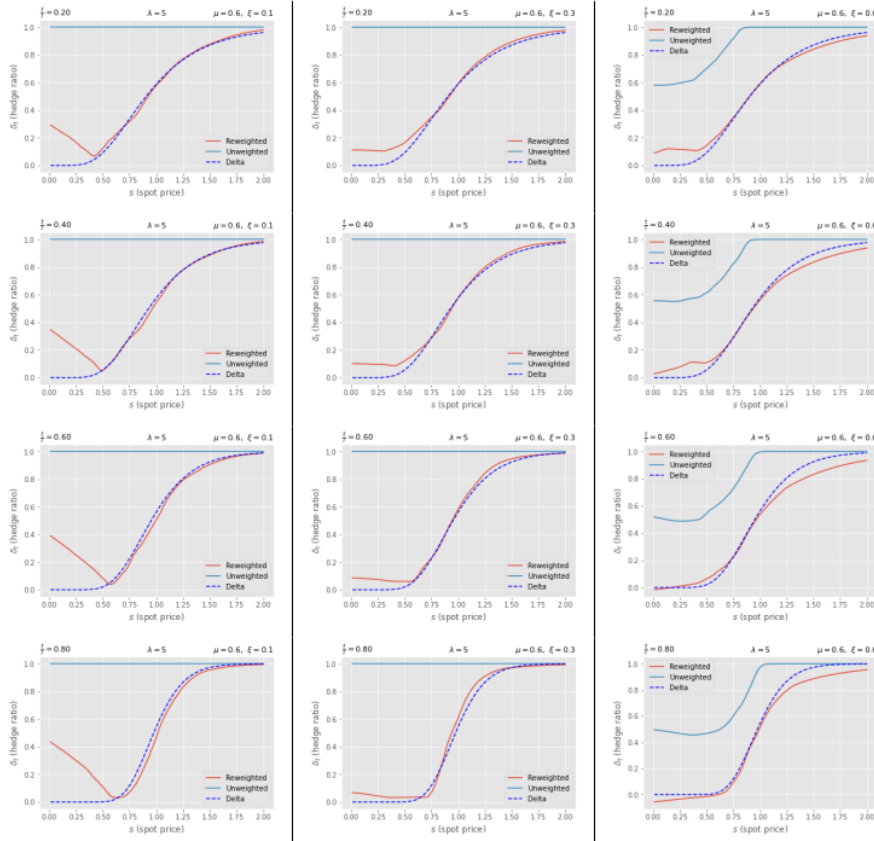


Figure A.37: Heston model - Hedge European call option with $\mu = 0.6$, $\lambda = 5$ and different positive volatility of instantaneous volatility ξ .

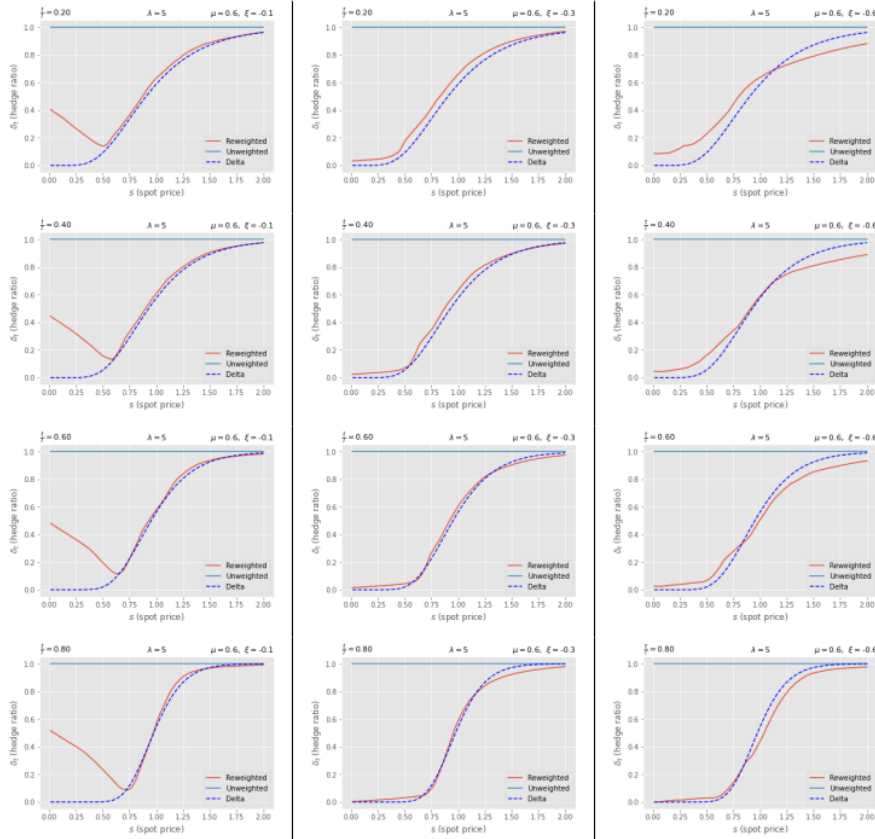


Figure A.38: Heston model - Hedge European call option with $\mu = 0.6$, $\lambda = 5$ and different negative volatility of instantaneous volatility ξ .

Bibliography

- [1] Alex, T. (2021). A Crash Course in Stochastic Analysis, *Lecture notes*.
- [2] B. Horvath, A. Muguruza Gonzalez and M. S. Pakkanen (2021): Harnessing quantitative finance by data-centric methods. In A. Capponi and C.-A. Lehalle (eds): *Machine Learning in Financial Markets: A Guide to Contemporary Practice*, Cambridge University Press, to appear.
- [3] Benhamou, E., Saltiel, D., Ungari, S. and Mukhopadhyay, A. (2020). Time your hedge with deep reinforcement learning. *arXiv preprint arXiv:2009.14136*.
- [4] Black, F. and Scholes, M. (2001). The Pricing of Options and Corporate. *Options Markets*, 1, 92.
- [5] Branger, N. and Schlag, C. (2008). Can Tests Based on Option Hedging Errors Correctly Identify Volatility Risk Premia? *Journal of Financial and Quantitative Analysis*, 43(4), 1055-1090. doi:10.1017/S0022109000014447
- [6] Broodryk, R. (2020). *The Lifted Heston Stochastic Volatility Model* (Master's thesis, Faculty of Commerce)
- [7] Buehler, H., Gonon, L., Teichmann, J. and Wood, B. (2019). Deep hedging. *Quantitative Finance*, 19(8), 1271-1291.
- [8] Buehler, H., Phillip, M., Pakkanen, M. and Wood, B. (2021). Deep Hedging: Learning Risk-Neutral Implied Volatility Dynamics. *Available at SSRN 3808555*.
- [9] Haugh, M. (2016). The Black-Scholes Model, *Notes.*, from url-<https://www.coursehero.com/file/32297035/BlackScholespdf/>
- [10] Heston, S. L. (1993). A closed-form solution for options with stochastic volatility with applications to bond and currency options. *The review of financial studies*, 6(2), 327-343
- [11] Howell, S. D. (2008). What a delta hedge really does—a theoretical and pedagogical note. *The European Journal of Finance*, 14(1), 33-47.
- [12] Huber, C. (2019). Machine Learning for Hedge Fund Selection. *Wilmott*, 2019(100), 74-81.
- [13] Kahneman, D. (2011). *Thinking, fast and slow*. New York: Farrar, Straus and Giroux.

- [14] Lalley, S. (2021). Lecture 7: The Black-Scholes Formula. Retrieved 6 September 2021, from <http://galton.uchicago.edu/~lalley/Courses/390/Lecture7.pdf>
- [15] LOBSTER — high quality limit order book data. (2021). Retrieved 6 September 2021, from <https://lobsterdata.com/>
- [16] MacBeth, J. D. and Merville, L. J. (1979). An empirical examination of the Black-Scholes call option pricing model. *The journal of finance*, 34(5), 1173-1186.
- [17] MacKinnon, J.G. (1994) “Approximate Asymptotic Distribution Functions for Unit-Root and Cointegration Tests.” *Journal of Business & Economics Statistics*, 12.2, 167-76.
- [18] Pakkanen, M. (2020). Deep Learning, *Lecture notes*.
- [19] Privault, N. (2021). Notes on Stochastic Finance., *Lecture notes*., from <https://personal.ntu.edu.sg/nprivault/MA5182/martingale-pricing-hedging.pdf>
- [20] Rutkowski, M. (2014). The Black-Scholes Model. *School of Mathematics and Statistics University of Sydney* Lalley, S. (2021). Lecture 7: The Black-Scholes Formula. Lecture notes, from http://www.maths.usyd.edu.au/u/UG/SM/MATH3075/r/Slides_8_Black_Scholes_Model.pdf
- [21] Wu, W., Chen, J., Yang, Z. and Tindall, M. L. (2021). A cross-sectional machine learning approach for hedge fund return prediction and selection. *Management Science*, 67(7), 4577-4601.

GRADEMARK REPORT

FINAL GRADE

/0

GENERAL COMMENTS

Instructor

PAGE 1

PAGE 2

PAGE 3

PAGE 4

PAGE 5

PAGE 6

PAGE 7

PAGE 8

PAGE 9

PAGE 10

PAGE 11

PAGE 12

PAGE 13

PAGE 14

PAGE 15

PAGE 16

PAGE 17

PAGE 18

PAGE 19

PAGE 20

PAGE 21

PAGE 22

PAGE 23

PAGE 24

PAGE 25

PAGE 26

PAGE 27

PAGE 28

PAGE 29

PAGE 30

PAGE 31

PAGE 32

PAGE 33

PAGE 34

PAGE 35

PAGE 36

PAGE 37

PAGE 38

PAGE 39

PAGE 40

PAGE 41

PAGE 42

PAGE 43

PAGE 44

PAGE 45

PAGE 46

PAGE 47

PAGE 48

PAGE 49

PAGE 50

PAGE 51

PAGE 52

PAGE 53

PAGE 54

PAGE 55

PAGE 56

PAGE 57

PAGE 58

PAGE 59

PAGE 60

PAGE 61

PAGE 62

PAGE 63

PAGE 64

PAGE 65

PAGE 66

PAGE 67

PAGE 68

PAGE 69

PAGE 70

PAGE 71

PAGE 72

PAGE 73

PAGE 74

PAGE 75

PAGE 76

PAGE 77

PAGE 78

PAGE 79

PAGE 80

PAGE 81

PAGE 82

PAGE 83

PAGE 84

PAGE 85

PAGE 86

PAGE 87

PAGE 88

PAGE 89
